The Last Scandinavian Ice Sheet in Wielkopolska and Mid-Holocene Meteorite Impact Craters

Field Guide

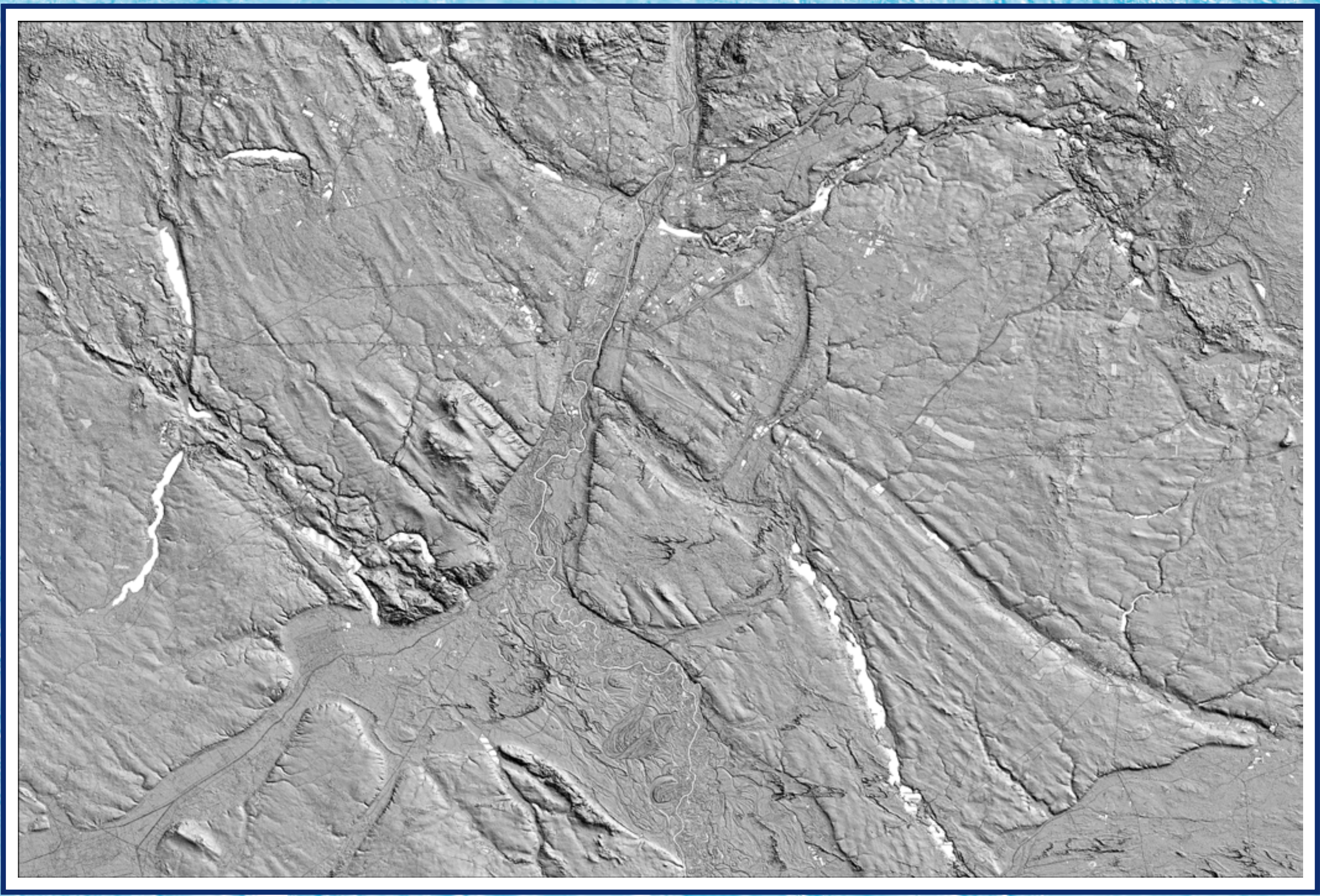

1st International Conference
'Processes and Palaeo-environmental changes in the Arctic: from past to present' (PalaeoArc)

Adam Mickiewicz University, Poznań, Poland

Poznań, 20–24 May 2019

Adam Mickiewicz University, Poznań

The Last Scandinavian Ice Sheet in Wielkopolska and Mid-Holocene Meteorite Impact Craters

Field Guide

Izabela Szuman-Kalita
Marek Ewertowski
Jakub Kalita
Leszek Kasprzak
Mirosław Makohonienko
Krzysztof Pleskot
Witold Szczuciński
Aleksandra Tomczyk

Faculty of Geographical and Geological Sciences
Adam Mickiewicz University, Poznań

Poznań 2019

ISBN 978-83-7986-243-6

Printed in Poland by:
Bogucki Wydawnictwo Naukowe
ul. Górna Wilda 90, 61-576 Poznań
tel. +48 61 8336580
e-mail: bogucki@bogucki.com.pl
www.bogucki.com.pl

Contents

Izabela Szuman-Kalita, Marek Ewertowski, Jakub Kalita, Leszek Kasprzak, Aleksandra Tomczyk

1. The Last Scandinavian Ice Sheet in Wielkopolska – Introduction

The margin of the last Scandinavian Ice Sheet (SIS) attained its farthest southernmost position during Vistulian (Weichselian) in western Poland and eastern Germany, advancing slightly south of latitude 52°N (**Figure 1A**). During the fieldtrip, we will visit several sites in Wielkopolska, focusing on the dynamics of SIS in this area. The exact chronology of glacial events is still somewhat unclear, but the Last Glacial Maximum (LGM) in the area can be placed at c. 20 ka BP (Kozarski, 1986, 1995a) or c. 24 ka BP (Marks, 2002, 2010). The farthest southern line of the ice advance is known as the Leszno (Brandenburger) Phase, and the subsequent retreat phase c. 18.8–20 kaBP (18.8 after Kozarski, 1995a; 20 ka BP after Marks, 2002, 2010) is called the Poznań (Frankfurter) Phase (**Figure 1B**).

The youngest geological cover in the western part of the Polish Lowland consists of Cenozoic sediments, represented by marine (Tetyda Ocean) sediments from Eocene-Oligoceneand terrestrial deposits in the Miocene epoch (Krygowski, 1961). Both sequences are composed of clays, sands, gravels, and coal. The Miocene sequence is overlaid with thick Pliocene clays (Poznań clay formation; Krygowski, 1961). As such, the Pleistocene ice sheets in central west Poland advanced over a thick, weakly permeable substratum, which had important implications for ice sheet dynamics. Close to the Leszno Phase, and near Leszno and Gostyń, Tertiary clays form a ramp, with the highest elevated surface along the LGM margin, and the surface of clays dipping gently toward the north but steeper toward the south (Augustowski, 1956; Kasprzak and Kozarski, 1991; Krzyszkowski and Gratzke, 1994). The Elsterian till constitutes the first regular widespread Pleistocene horizon in Wielkopolska (Czerwonka and Krzyszkowski, 1994; Czerwonka, 2004). The sediments associated with Saalian glaciation are fragmented, but the Saalian till can in places achieve significant thickness of 60 to 70 m (Kozarski, 1991). The Weichselian till horizon is much thinner, usually below c. 7 m (Krygowski, 1975) with a maximum of up to c. 22 m (Krygowski, 1952; Kozarski, 1991). According to several studies (Krygowski, 1975; Kozarski, 1991, 1992; Górska, 1995; Górska, 2000), only one subglacial Weichselian till horizon was recognised in Wielkopolska, albeit still currently being verified.

As already mentioned, the chronology of the Weichselian glacial events in central western Poland remains largely uncertain. Previously, recognition of glacial events in central western Poland has focused mainly on lithological and morphological criteria, (e.g. Woldstedt, 1925, 1954; Krygowski, 1961, 1967, 1972, 1975). One of the first studies to use absolute dating has suggested the age of the maximum extent of glaciation in Poland for 21-20 ka BP, based on C-14 dates (Cepek, 1965). Other publications have also corroborated this first study (Tobolski and Mojski, 1979b, a; Pazdur et al., 1980; Stankowska and Stankowski, 1988). A more modern stratigraphy of the Weichselian was based on further C-14 and new litho- and morpho-stratigraphic studies. New datings for the specified phases were proposed during the 1980s based on new C-14 dates: Leszno phase: ~20 ka BP (Kozarski, 1986); 20.5 ± 0.5 ka BP (Rotnicki and Borówka, 1989); 18.8 ka BP (Liszkowski, 1987); Poznań phase: 18.4 ka BP (Kozarski, 1986); 17.6 ka BP (Liszkowski, 1987). The mean annual retreat rate of the ice sheet was calculated to be 51 m a^{-1} (Kozarski, 1995a). The assumption that the maximum extent of the main stage in Wielkopolska did not take place any earlier than about 21 ka (Stankowska and Stankowski, 1988, 1991; Stankowski, 2000) is based on the TL dating of the deposits in the Konin region. Recently, new dates based on OSL and terrestrial cosmogenic nuclide (TCN) dating have been provided for Poland by Marks (Marks, 2012) and Rinterknecht et al. (2005) among others, but these are based on samples located outside Wielkopolska. Still, a very small number of sites in western Poland have been dated using OSL and/or TCN, and thus this region represents a gap between Germany, eastern and northern Poland. An extrapolation of the data from Germany (Heine et al., 2009; Lüthgens et al., 2010; Luthgens et al., 2011; Rinterknecht et al., 2014) and other parts of Poland is only possible to a very limited extent, because the dynamics of the ice sheet's margin varied greatly in different regions (Rinterknecht et al., 2014). Moreover, most of the

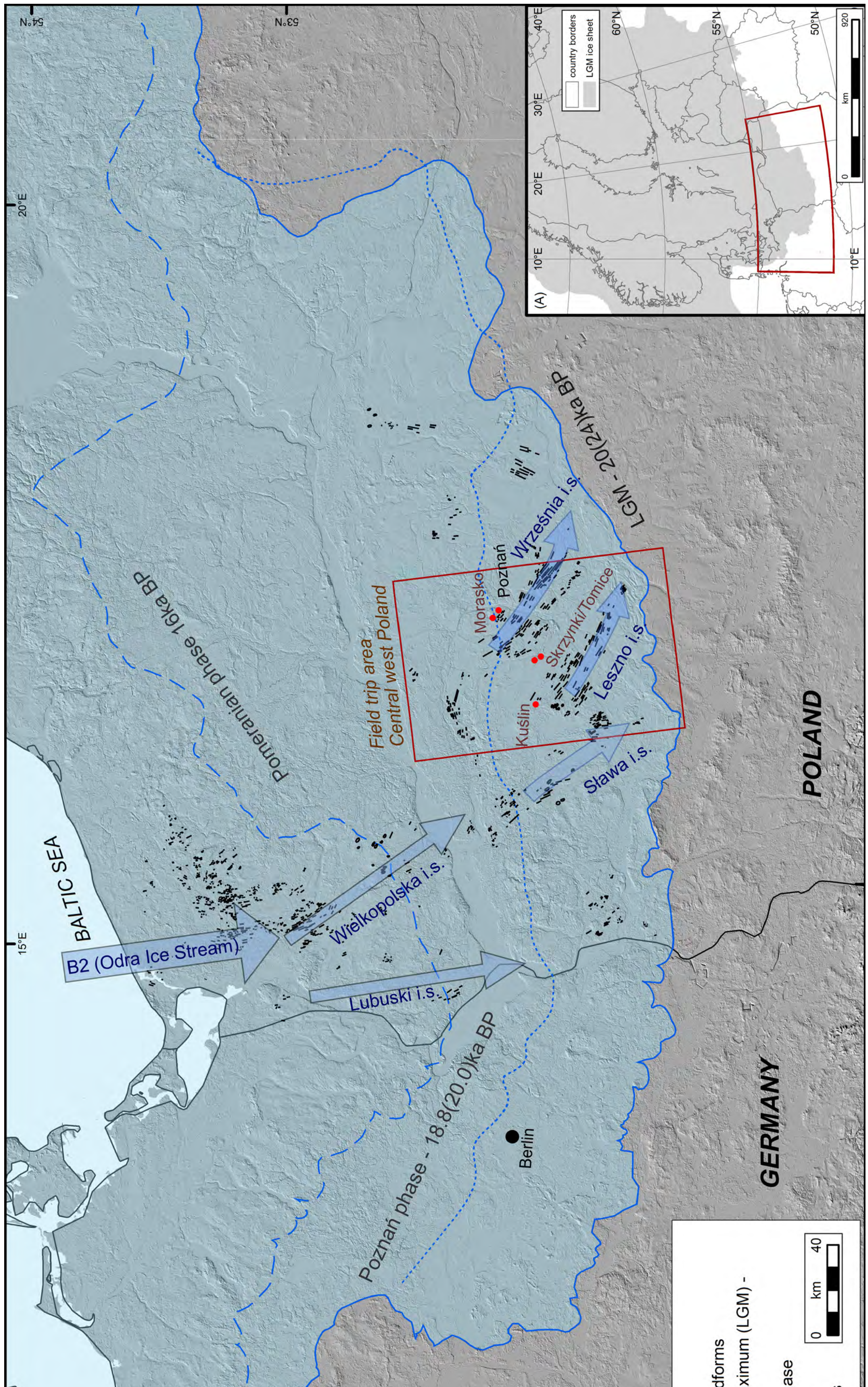

Figure 1. Location of the study area: (A) the overview map shows the extent of the Weichselian ice sheet in northern Europe; (B) limits of the main phases of the Weichselian glaciation in Poland in terms of time and extent (after Kozarski, 1995) and location of the main ice-streams. The figure was modified from Szuman et al. (2018).

above-mentioned dates were related to the deglaciation periods. Much less attention has been paid to the timing during the advance of the Weichselian ice sheet, hence the advance velocity not being well-known. In 2016, we embarked on a research project entitled 'Reconstruction of glacial history in central west Poland during the Weichselian glaciation' (PI: Izabela Szuman-Kalita), aimed at examining the timing of advance and decay of the SIS during Weichselian in central west Poland based on extensive OSL and TCN dating. Therefore, in the next couple of years, our knowledge of glacial chronology in those areas should improve.

1.1. Dynamics of the Weichselian ice sheet in central west Poland – geomorphological background

The lobate shape of the LGM margin was related to the activity of the palaeo-ice streams, whose occurrence was interpreted through satellite image analyses by Punkari (1997). According to those investigations, during the Weichselian glaciation SIS over Poland was drained by two branches of the Baltic ice stream: B2 and B3 (Punkari, 1997; Boulton et al., 2001), also known as the Odra and Wisła ice streams respectively (Marks, 2010), and while the area of Wielkopolska was in the inter-stream zone. More recent studies by Kasprzak (2003) and Przybylski (2008) applied sedimentological and morphological criteria to distinguish the three smaller branches of the Odra ice stream in Wielkopolska: Września, Leszno, and Sława Śląska ice lobes. However, the increased availability of high-resolution remote sensing products and digital elevation models has permitted a more detailed mapping of the glacial landform in a regional scale for the area of west Poland, thus making it possible to propose a new and more detailed interpretation. Recent works concerning the marginal part of the Odra ice-stream (Przybylski, 2008; Szuman et al., 2013; Spagnolo et al., 2016), or including it as a boundary region for the analyses (Wysota et al., 2009; Roman, 2017), took into account the occurrence of mega-scale glacial lineations (MSGLs) and a dynamic perspective of the ice masses' activity, and revised ice stream patterns proposed by Punkari (1997) and Boulton et al. (2001).

We enhanced the former approach and mapped a large number of new, previously unrecognized streamlined features in the southern sector of SIS across west Poland. The basic dataset comprised a high-resolution LIDAR point cloud that enabled the generation of a digital elevation model (DEM) with a 0.4 m ground sampling distance. Our investigations revealed for the first time a wide variety of streamlined bedform types. These features occupied especially the area of north east Poland in the lower Odra region (see Hermanowski et al., 2019 for details), and the extensive topographic lowering restricted from the east by Gniezno moraines complexes and from the west by Lubusz elevation. We recognised several flow-sets and some single ridges indicating the existence of highly dynamic ice streams in this region instead of slow-moving ice within the inter-stream zone. Based on the distribution of flow-sets, we suggested an updated inventory of ice streams in west Poland.

1.2. A new pattern of ice streams in west Poland

The Odra ice stream in the lower Odra valley was divided into the Wielkopolski ice stream that reached central Poland, extending up to the Jarocin-Pleszew area, the Lubuski ice stream to the west, and the rest of the ice mass across north eastern Germany. Based on the distribution of streamlined bedforms and the sedimentological evidence, we suggest that the main ice flux of the Odra ice stream (*sensu* Marks, 2010) advanced toward the southeast, along the Wielkopolska ice stream thus. Our analysis does not confirm the concept presented by Punkari (1997), who suggested that the main ice mass flowed south-westward. The Wielkopolska ice stream further split into two branches: Września and Leszno-Sława ice stream. The latter was again divided into two smaller branches (Leszno and Sława) at around the higher elevated Lwówek-Rakoniewice rampart (**Figure 1**), as indicated by Przybylski (2008).

The streamlined bedforms found along the ice steams in Wielkopolska are typically mega-scale glacial lineations, drumlins and smaller flute-like features. MSGLs are usually 1–4 m high (mean

c. 2 m), with a main orientation of NW-SE (details of MSGLs along the Września ice stream can be found in Spagnolo et al., 2016). The length of the forms is difficult to measure because of human activity, meltwater erosion, and aeolian processes. Nevertheless, they are up to 8.5 km long. The drumlins have an average length of c. 700 m and a height of 3 to 9 m. The small flute-like features are difficult to analyse morphometrically due to the aeolian cover, but their height is c. 0.7 m.

The full population and precise dimensions of the palaeo-ice streams in this southern sector of the SIS are yet to be determined. However, the overall highly dynamic nature of the ice masses in this sector can be explained, at least in part by the influence of the geothermal heat flux's high values (Section 1.3).

1.3. The relationship between geothermal heat flux and the last Scandinavian ice sheet dynamics

Geothermal heat flux (GHF) is heat that is supplied to the base of the ice sheet. It plays an important role in controlling ice sheet stability, and affects basal temperatures, melting, and ice flow velocities. In a study by Szuman et al. (2018), we suggested that the high GHF might have been one of the factors influencing the last SIS's behaviour in its southernmost sector.

Our data sources included maps of the heat flow density and temperature at a depth of 2000 m. For Poland, we used the geothermal heat flow map published by Szewczyk and Gientka (2009), and for Germany the data from the Global Heatflow database was used (at the International Heat Flow Commission: http://engineering.und.edu/geology-and-geological-engineering/globe-heat-flow-database; Abdulmalik (2015)). In addition, we used a temperature map at a 2000-metre depth for Poland (Szewczyk, 2010) and Germany (LIAG, 2015), as the values for this depth are assumed to be free from the effects of surface temperatures (Szewczyk and Gientka, 2009).

The GHF in western Poland reached even more than 100 mW m^{-2} (**Figure 2A**), which is much higher than that in eastern Poland, where GHF was <40 mW m^{-2} (Szewczyk and Gientka 2009). A similar trend was found for temperature values at a depth of 2000 m (**Figure 2B**).

For the analysed case, a GHF of 80 mW m^{-2} approximates the level of upward heat conduction. The difference in basal temperatures between areas with higher and lower GHF due to ice insulation was about 3–4°C (**Figure 3A, B**). Such a difference could either increase the basal melting or facilitate achieving the pressure melting point. The results of the upward heat conduction (G) for ice thickness H = 300 m and surface temperature T = –8°C (French 2007, p. 316) show that G min = 60 mW m^{-2} is probable for the SIS in the area of central west Poland (**Figure 3C**). Any excesses in GHF would lead to an increase in the basal melting rate. If the ice thickness was 300 m or more, the significance of the GHF would be higher and with less uncertainty. The difference between the plots for vertical advection of 5 and 10 cm per year shows that the upward heat conduction is not that sensitive to the vertical advection parameter for the analysed case.

The shearing heat generation for fast moving ice streams (at least 500 ma^{-1}), with a low surface slope of 0.4×10^{-3} and protruding over a relatively flat area with a well-lubricated bed, was calculated to be below 15 mW m^{-2} (for details, see Szuman et al., 2018). In the case of GHF values of 80–100 mW m^{-2}, we obtained 8–10 mm of meltwater from GHF. The difference in melt rates between GHF of 40 and 80 mW m^{-2} is about 4 mm. An additional 2 mm of meltwater was generated from shear heating of 15 mW m^{-2}. Therefore, the meltwater production along the axial part was dominated by GHF and can potentially have significant impact on ice sheet dynamics.

Based on the modelling results, we suggested that the high GHF contributed to the intense meltwater production (Szuman et al., 2018). The water was at least partly stored subglacially due to the low-permeable bed and lack of channelized drainage traces. The presence of elevated GHF maintained a fast ice streaming over the gentle topography in central west Poland. In such a case, a fast-moving ice stream over a well-lubricated bed could have been in a delicate thermal balance (**Figure 3D**) – this fast ice flow is confirmed by the occurrence of MGSLs (Section 1.1) and sedimentary structures visible in the outcrops (Szuman et al., 2013).

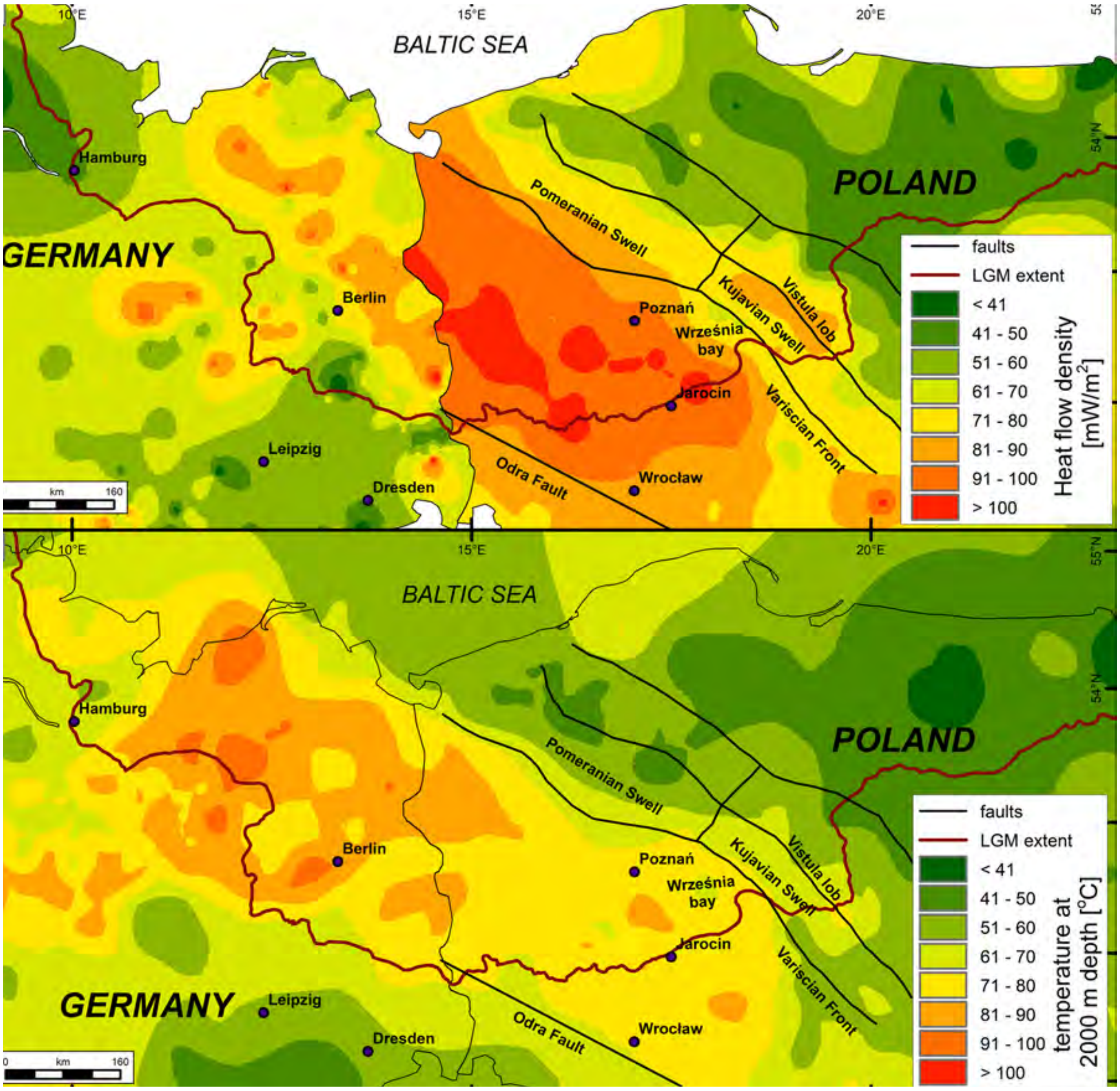

Figure 2. (A) Geothermal heat flow based on Szewczyk and Gientka (2009) and Global Heatflow database; and (B) temperature at a depth of 2000 m based on Szewczyk (2010) and LIAG (2015) in NW Poland and NE Germany. Reproduced from Szuman et al., 2018 – The impact of geothermal heat flux on the last Scandinavian ice sheet over W Poland and E Germany. Geografiska Annaler: Series A, Physical Geography, 100(4):388–403 reprinted by permission of the publisher (Taylor & Francis Ltd, http://www.tandfonline.com).

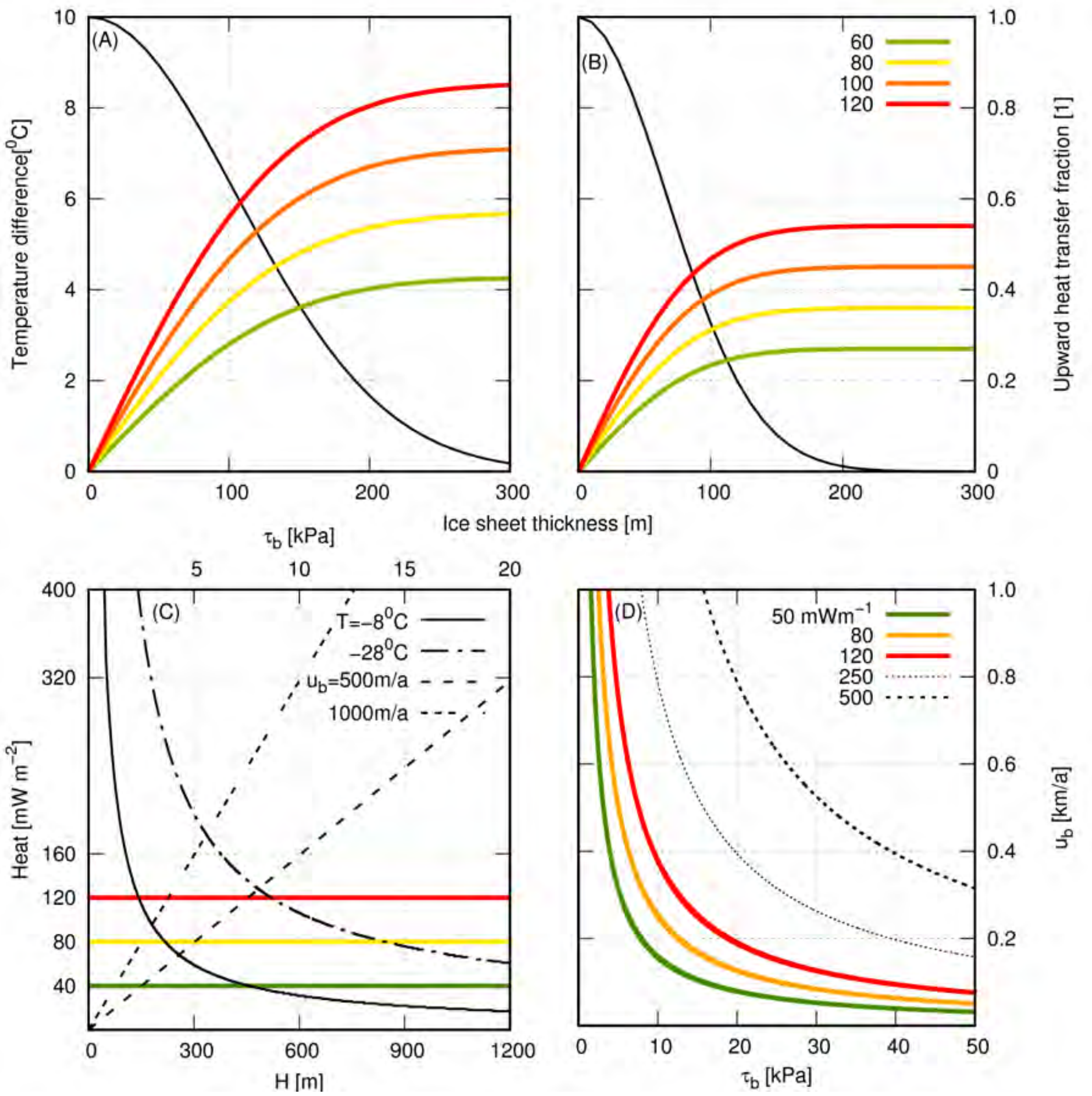

Figure 3. Differences in temperature between the base of the ice and distance in the direction of the surface h for annual accumulation values of (A) 250 mm and (B) 100 mm; second scale (right) indicates the fraction of the upward heat transfer at height h above the base of the ice sheet; (C) an upward heat conduction in ice sheeet thickness for surface temperatures T = –8°C and –28°C (corresponding to the SIS LGM and current Antarctic mean annual temperatures, respectively) and heat generation due to basal shear stress ($\tau_{b,}$ – top scale) for basal velocities u_b = 500 and 1000 m a^{-1} as probable for the analysed ice stream; co-horizontal lines show low (40 mW m^{-2}), average (80 mW m^{-2}), and high (120 mW m^{-2}) GHF values for the analysed region; (D) the relation between basal shear stress and velocity with a constant value of generated heat. Less heat makes the balance state more sensitive to changes in the conditions. Modified from Szuman et al. (2018).

1.4. Development of permafrost after SIS retreat

In a study by Ewertowski et al. (2017), we described the occurrence of numerous cropmarks (< 400 sites) in central west Poland (**Figure 4**). Their geometry and distribution were studied using a large number of low-altitude aerial photographs. Based on the field verification, we interpreted them as past thermal-contraction-cracks, filled with aeolian sand (i.e. sand-wedge casts). We identified seven principal types of polygon geometry based on the angle of the cracks' intersection, their dimension and spacing: Type A – large, irregular, orthogonal polygons (**Figure 5A**); Type B – small, irregular, orthogonal polygons (**Figure 5B**); Type C – regular, orthogonal polygons (**Figure 5C**); Type D – irregular, non-orthogonal polygons (**Figure 5D**); Type E – regular, non-orthogonal polygons (**Figure 5E**); Type F – mixed, orthogonal, and non-orthogonal polygons (**Figure 5F**); Type G – incomplete polygons.

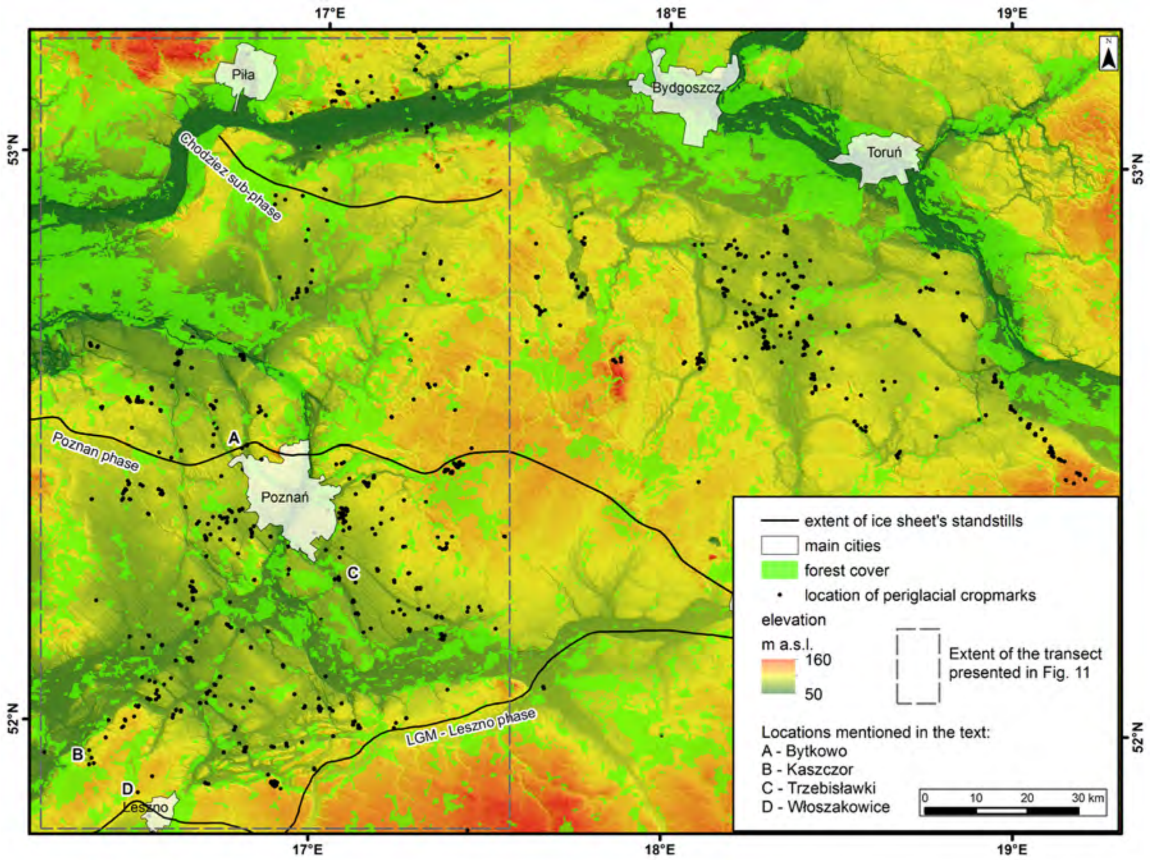

Figure 4. Distribution of polygonal nets in central west Poland. Reprinted from Geomorphology, 293, Ewertowski et al, Low-altitude remote sensing and GIS-based analysis of cropmarks: Classification of past thermal-contraction-crack polygons in central western Poland, Pages 418–432., Copyright (2017), with permission from Elsevier.

1.5. Relationship between the ice sheet's extent and geometry of polygonal nets

Many previous studies, (e.g Kozarski, 1995a, b; Kasprzak, 2003; Ewertowski, 2009), have suggested that permafrost aggraded gradually following the frontal recession of SIS's margin from the LGM extent. Hence, we assumed that:

1) The older the polygonal nets, the better they are developed, i.e. they are characterised by a complex structure, with the large primary polygons divided into smaller secondary and tertiary cracks (e.g. Type F).
2) The oldest well-developed polygonal nets should occur to the south of our study area near the LGM extent from where the ice sheet retreated earlier (e.g. Type F).

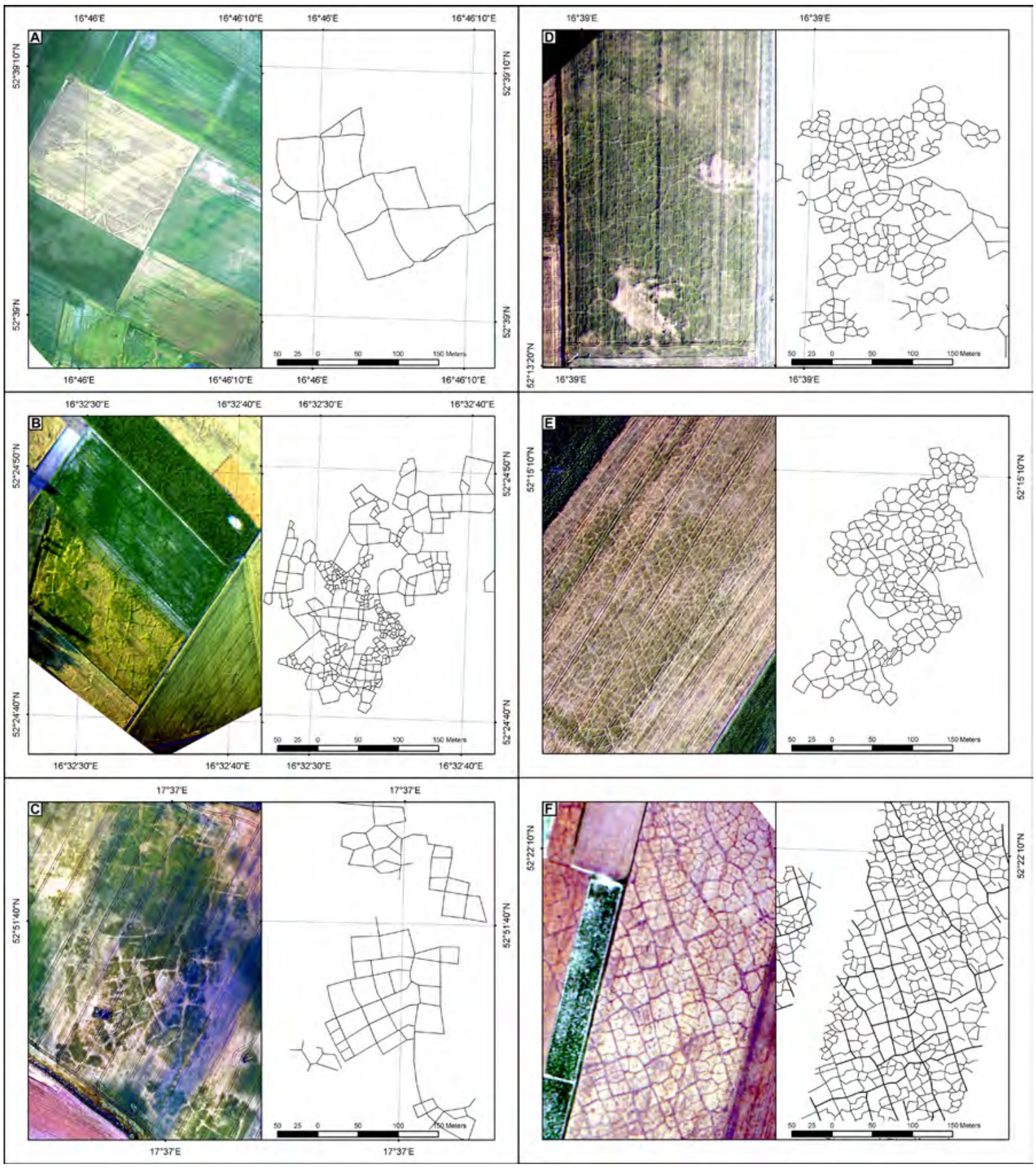

Figure 5. Examples of different types of periglacial cropmarks in Wielkopolska: (A) Type A – net of large, irregular, orthogonal polygons; (B) Type B – net of complex, small, irregular, orthogonal polygons; (C) Type C – regular, orthogonal polygons; (D) Type D – irregular, non-orthogonal polygons; (E) Type E – regular, non-orthogonal polygons; (F) Type F – mixed, orthogonal, and non-orthogonal polygons. Modified from Ewertowski et al., 2017.

3) The youngest polygonal nets should occur to the north of our study area and be characterised by less developed polygonal nets, i.e. simpler polygons (Type A) should be found closer to the Chodziez subphase.

We expected the polygons from the northern part of the study area to be less developed than those from the southern part, as they had less time to evolve due to the shorter period under periglacial conditions. In order to test this hypothesis, we selected a group of polygonal nets in the S-N transects, i.e. from the LGM margin toward the Chodziez subphase that developed under the same lithological and geomorphological conditions (i.e. within till plains), and then investigated their geometry.

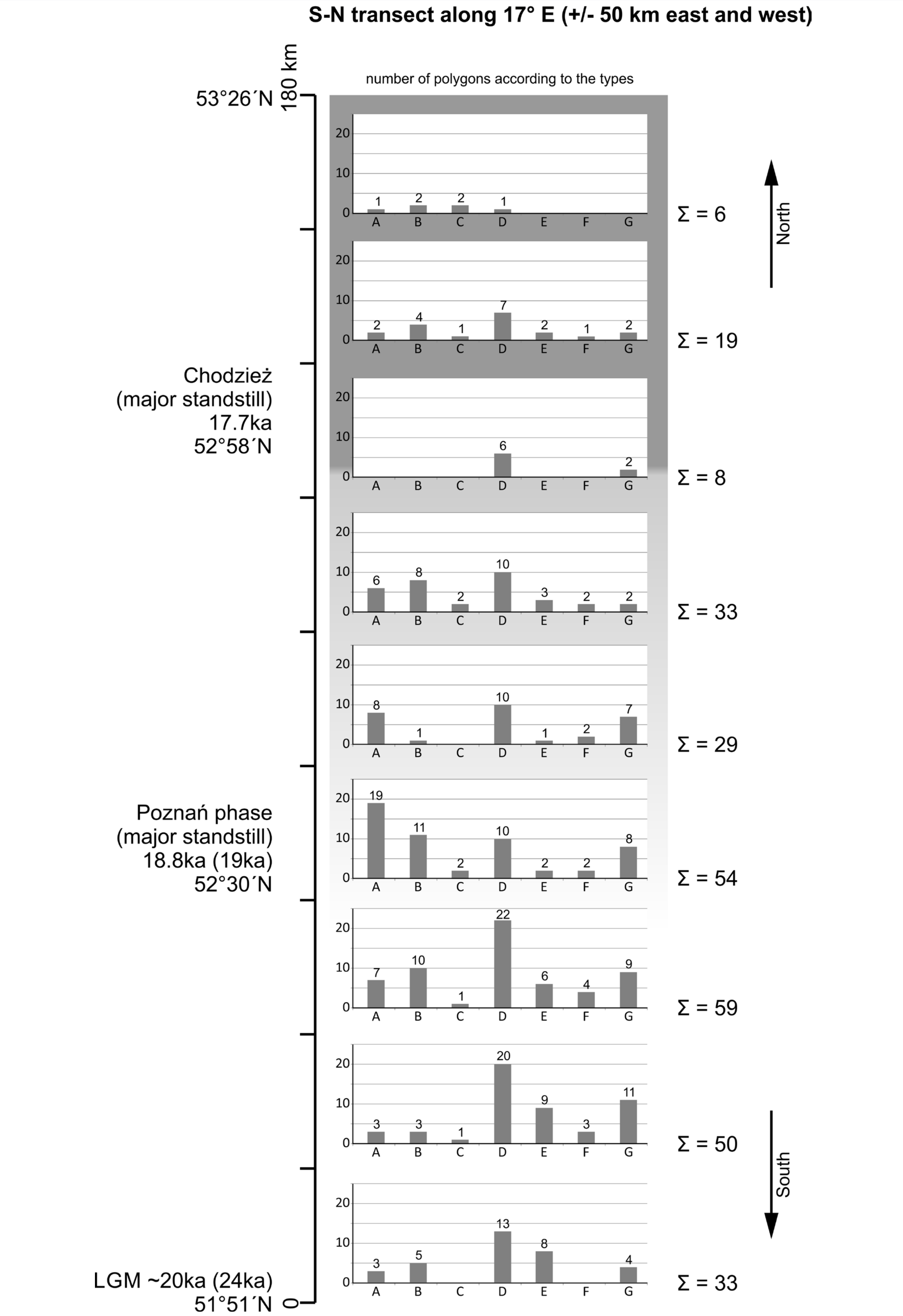

Figure 6. Relationship between polygonal nets' geometry and distance from the LGM to the north. Nets were counted in belts 100 km wide in W-E direction and 20 km long in N-E direction. Axis of the transect is 17°E. Reprinted from Geomorphology, 293, Ewertowski et al, Low-altitude remote sensing and GIS-based analysis of cropmarks: Classification of past thermal-contraction-crack polygons in central western Poland, Pages 418–432., Copyright (2017), with permission from Elsevier.

We were not able to confirm the expected relationship. The development of a specific type of polygons seemed unrelated to their geographic location, at least as far as the studied transect was concerned (**Figure 6**). Besides, the general distribution of geometrical types does not exhibit a strong relationship with the time of deglaciation. We did not find a higher accumulation of simple (i.e. initial) polygonal nets (type A) to the north or more complicated (i.e. more mature) ones to the south (types B–F). However, the total number of polygons was much lower in the northernmost part of the studied transect compared to the southern part (i.e. 33 polygon nets were found within the 60 km long northern part of the transect compared to 149 polygon nets observed for the 60 km long southern part) (**Figure 6**). This tendency could be an indication that in the northern part of the study area:

1) there were less thermal-contraction-cracking events due to change in climatic conditions as the ice sheet retreated to the north (i.e. occurrence of generally milder climatic conditions); or
2) local conditions were not generally as favourable for cracking as further south.

To sum up, the broad occurrence of polygons of former thermal-contraction-cracks filled with aeolian sediments (i.e. sand-wedge casts) indicated that continuous permafrost was widespread in central west Poland after the termination of LGM. However, their spatial distribution did not allow us to fully confirm the hypothesis regarding a gradual aggradation of the permafrost following the retreating ice margin. Preliminary dating of the cracks' infilling as well as polygon geometry suggest that thermal-contraction-cracking occurred in several different phases, and that a time frame of a few thousand years is enough to form even complex and mature nets.

This chapter is based on results of National Science Centre (Poland) grant No. 2015/17/D/ST10/01975.

Witold Szczuciński, Mirosław Makohonienko, Krzysztof Pleskot

2. Site I: Morasko Meteorite Nature Reserve

2.1. Introduction

The surfaces of Mercury, Mars or our own Moon are scarred by numerous impact craters, suggesting that collisions with planetoids and meteoroids are one of the most common geological processes in our solar system. Our own planet is no exception: we were reminded of this only recently, on 15 February 2013, when a meteorite struck near Chelyabinsk, injuring around 1,500 people and partly destroying 7,200 buildings. Although, there are many impact craters on Earth, they can be difficult to identify. This is mainly due to extensive erosion, sedimentation, and tectonic deformations taking place over long periods, all of which damage and destroy impact structures. The Earth Impact Database (www.passc.net/EarthImpactDatabase/) lists over 190 confirmed structures. One of them is a complex of impact craters near the village of Morasko, which falls within the administrative boundaries of the city of Poznań, western Poland (**Figure 7**). It is considered to be a site of the largest iron meteorite shower in Central Europe.

The Morasko Meteorite has already a 100 years long history of investigations. The first findings date back to 1914, when four meteorite pieces were found by dr. Cobliner while digging of military trenches. The weights of these meteorites were 77.5 kg, 4.2 kg and two pieces of 3.5 kg each. Up to now, almost 2,000 kg of extraterrestrial matter has been documented with particular pieces ranging in weight from a few grams to more than 260 kg. Apart from meteorites, there are also depressions, up to 100 m in diameter, interpreted already by Pokrzywnicki (1964) to be impact craters. The presence of both, extraterrestrial metallic material and the morphological effects of its fall, make

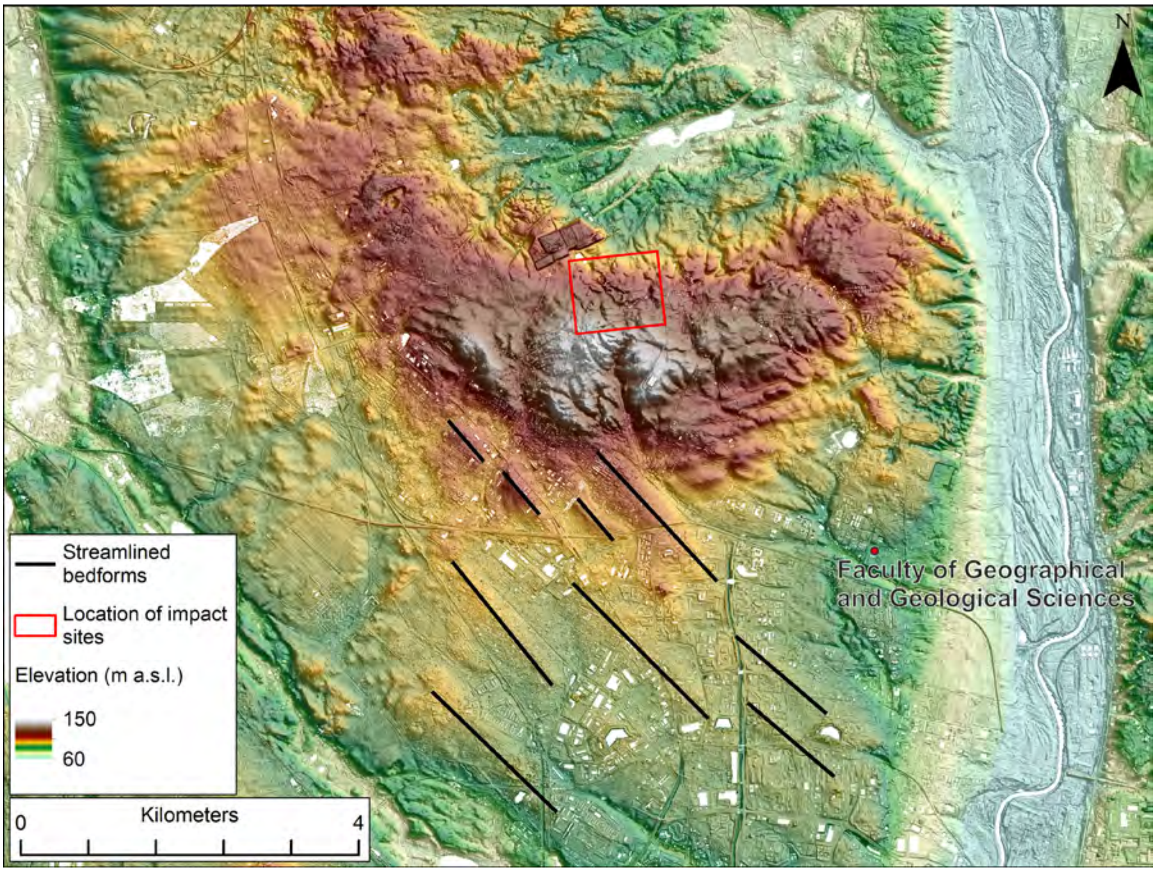

Figure 7. Location of the Morasko site.

the Morasko to be one from less than 20 documented sites worldwide, where the remnants of the impacting body are found next to the craters.

2.2 The geological and geomorphological context

The most of meteorite founds and the craters are within a belt of recessional moraines that developed ca. 18.5 thousand years ago during the Poznań phase (the Frankfurt phase) of the last glaciation (Karczewski, 1976; Chmal, 1990; Kozarski, 1995a; Stankowski, 2001; Stankowski, 2008). These moraines are built mainly of late Pleistocene glacial and glacifluvial sediments – till, sand and gravel – as well as of the glacio-tectonically deformed "Neogene clays" of the so-called Poznań series (**Figure 8**). The glacio-tectonic deformation had likely already developed during older glaciations (Chmal 1990; Stankowski 2008). In the neighbourhood of the moraines, many depressions have also formed as a result of the melting of dead ice blocks filling tunnel valleys or buried in glacifluvial sediments (Stankowski 2008). A number of depressions currently host lakes of various shapes and sizes, filled with lacustrine sediments deposited since the time of dead ice degradation several hundreds to a few thousand years after the ice sheet retreat (Pleskot et al., 2018).

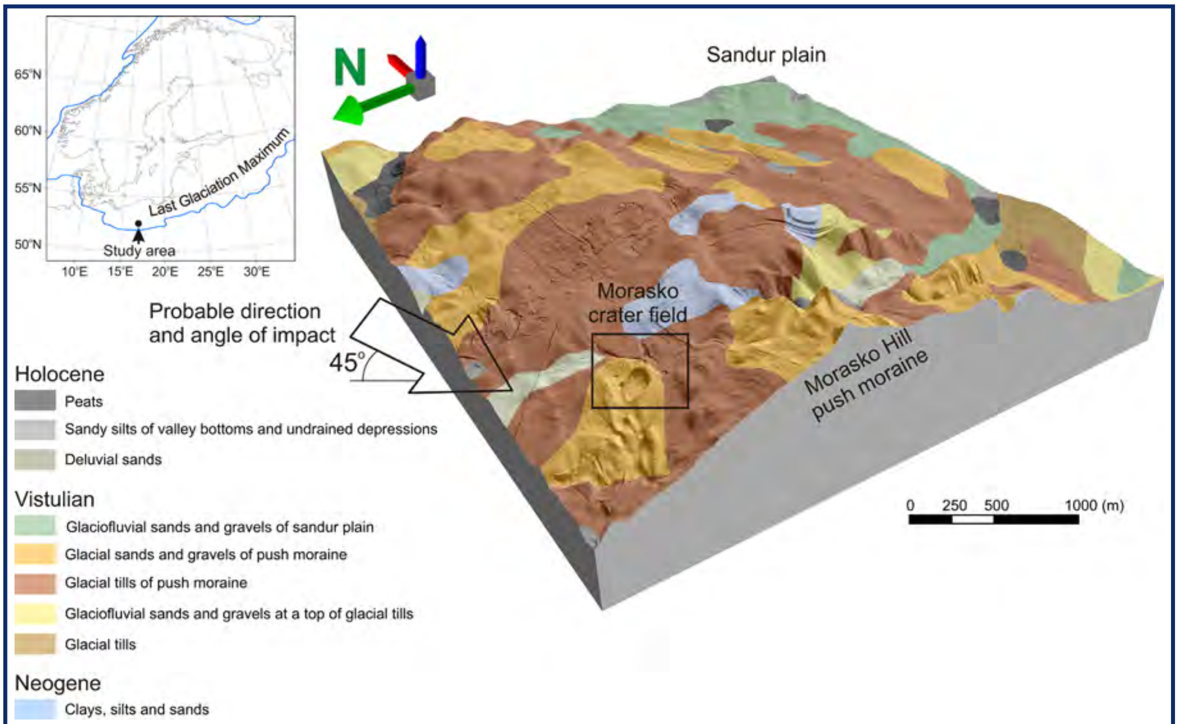

Figure 8. Geomorphological and geological setting of Morasko craters field. Block diagram showing surficial geology of the study area after the Detailed Geological Map of Poland (Chmal, 1990), draped on LiDAR-based DEM (note the north direction). An arrow marks the probable meteoroid impact from the NE direction at a dip angle of 45° (Muszyński et al., 2012; Bronikowska et al., 2017). Inset map shows position of the area in northern Europe. (Figure after Włodarski et al. (2017), Copyright: Elsevier – license number 4584740924765).

2.3. The meteorite

The Morasko meteorites have consistent chemical and mineral composition and their spatial distribution indicate that they originate from the disintegration of a single meteoroid (a "meteoroid" is a cosmic body, whereas a "meteorite" is the rock material left behind after meteoroid strikes the Earth). Meteorites are an invaluable source of information on the development of our solar system, the internal structure of planets and processes occurring in space. The extensive studies of the Morasko meteorite have resulted in many fascinating discoveries, the most important of which concern its composition. It is a coarse-grain octahedrite meteorite containing 7% nickel (Ni) and 93% iron (Fe) on average (Muszyński et al., 2012). The mineral composition is dominated by kamacite and taenite (alloy of Fe and Ni) and sporadic occurrence of cohenite and schreibersite (Fe and Ni calcites and phosphates). It also contains nodules with a diameter between 1 and 2.5 cm, comprising graphite and troilite with trace silicates, sulfates, oxides and phosphates (**Figure 9**). Recently, two new minerals known as moraskoite and czochralskiite – neither of which are found on Earth – have been discovered in the Morasko meteorite (Karwowski et al., 2015; 2016).

Figure 9. One of the biggest chunks (164 kg) of meteorite Morasko, exposed in museum of Faculty of Geographical and Geological Sciences of Adam Mickiewicz University in Poznań. This coarse-grain octahedrite (Muszyński et al. 2012) contains also rounded black nodules composed mainly of graphite and various trace compounds. Among the latter are also two new minerals discovered in the Morasko meteorite: moraskoite (Karwowski et al. 2015) and czochralskiite (Karwowski et al. 2016).

2.4. Craters

Not all meteorites cause the formation of impact craters. Many strike Earth's surface without causing significant damage, and even the very fact that they are responsible for impact craters had been questioned until relatively recently. Jerzy Pokrzywnicki, one of the first scholars of the Morasko meteorite in the mid-20th century, suggested that a few round depressions with a diameter of up to 100 meters (**Figure 10**), found on the slopes of moraine hills, are impact craters (1964). However, the identification of such relatively small structures was fraught with difficulties. Major impacts are responsible for extremely high temperatures and pressures which cause visible changes in rocks; the process is known as shock metamorphism. In more minor events, the conditions favoring the formation of craters may not be significantly different from other processes shaping Earth's surface. This was just one of the problems facing the researchers studying the Morasko craters. Rounded hollows are not unusual in post-glacial landscapes and they can be found in many locations in northern Poland as so called kettle holes.

In Morasko's case, it was the time of the ice sheet's retreat which provided the key to solve the problem of the origin of the round depressions. The largest crater is filled with water and its bottom is covered with sediment including plant remains which have been radiocarbon dated to being no older than 5,500 years. This suggests that their formation is significantly younger than the surrounding post-glacial landscape. The impact origin of the depressions is indicated by their

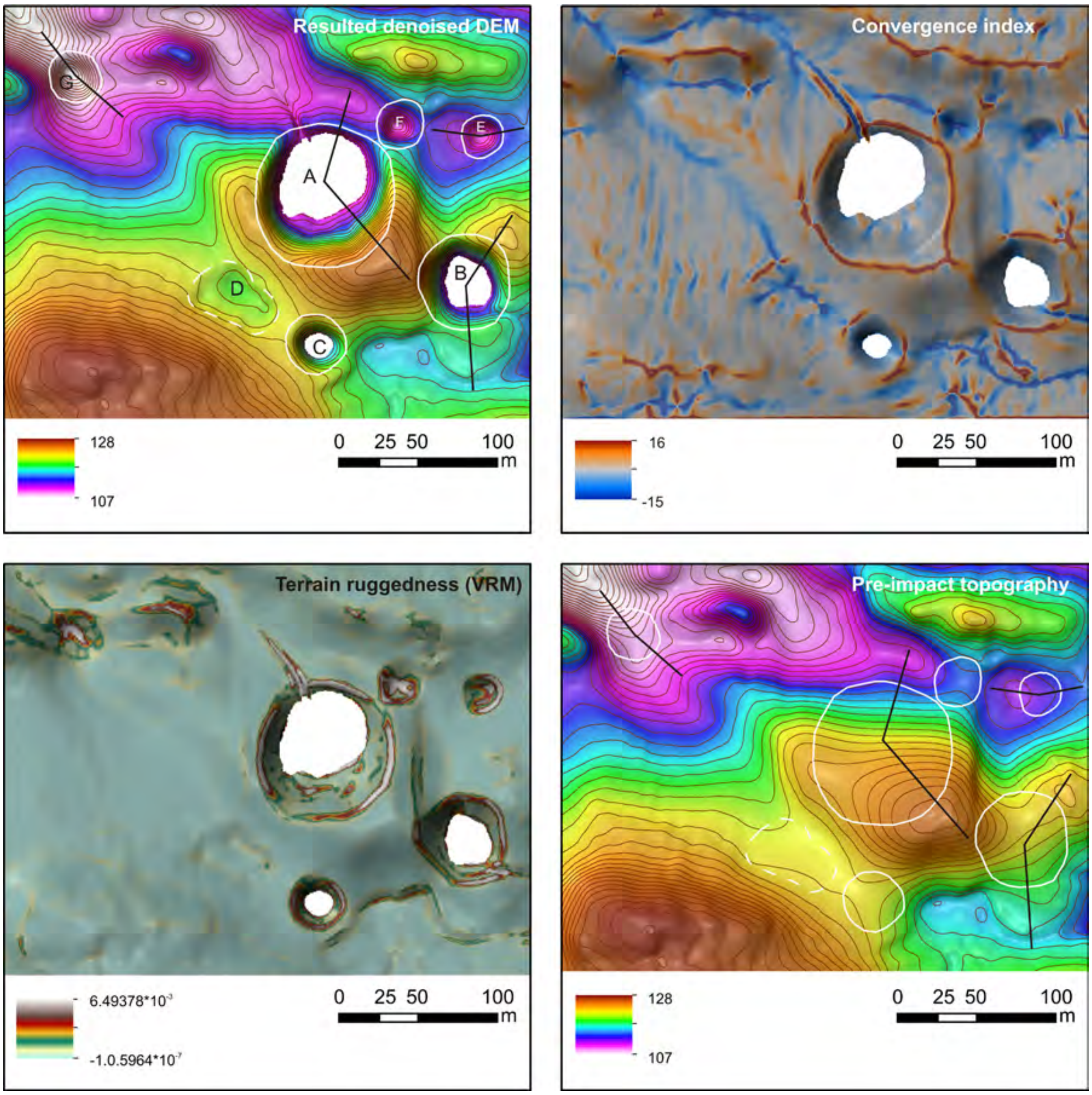

Figure 10. Final DEM and some of its derivative topographic attributes (slope convergence and terrain ruggedness), as well as reconstructed pre-impact topography. DEM and pre-impact topography are contoured at 5-m intervals. White lines mark boundaries of impact craters. The labels of craters used here are the same as those used in earlier studies (Pokrzywnicki, 1964, Karczewski, 1976, Stankowski, 2008). (Figure after Włodarski et al. (2017), Copyright: Elsevier – license number 4584740924765).

morphology (**Figure 10**), spatial distribution, age of sediment, findings of meteorites (**Figure 9**) and micrometeorites, and the recently documented sediment displaced from the craters and found in the surrounding area, called ejecta (Szokaluk et al. 2019, **Figures 11–13**). Initially it was interpreted as glacial sediment; however, it has since been found that it covered soil whose age matches that of the oldest sediments filling the craters – around 5,500 years (**Figure 12**). Geophysical, sedimentological and mineralogical research continues to provide data which makes it possible to interpret crater formation processes with increasing precision.

2.5. Environmental effects

Meteoroid strikes are rare and rapid, and they cannot be observed and measured in real time. The only way of gaining insight into the processes and the forces behind them is studying indirect evidence, such as crater size or shock metamorphism of rocks, as well as applying numerical modelling.

Numerical experiments based on available data conducted by Bronikowska et al. (2017) show that the meteoroid had an original mass between 600 and 1100 metric tons and moved at a speed between 16 and 18 km/s. It is likely to have disintegrated in the atmosphere; the largest crater was

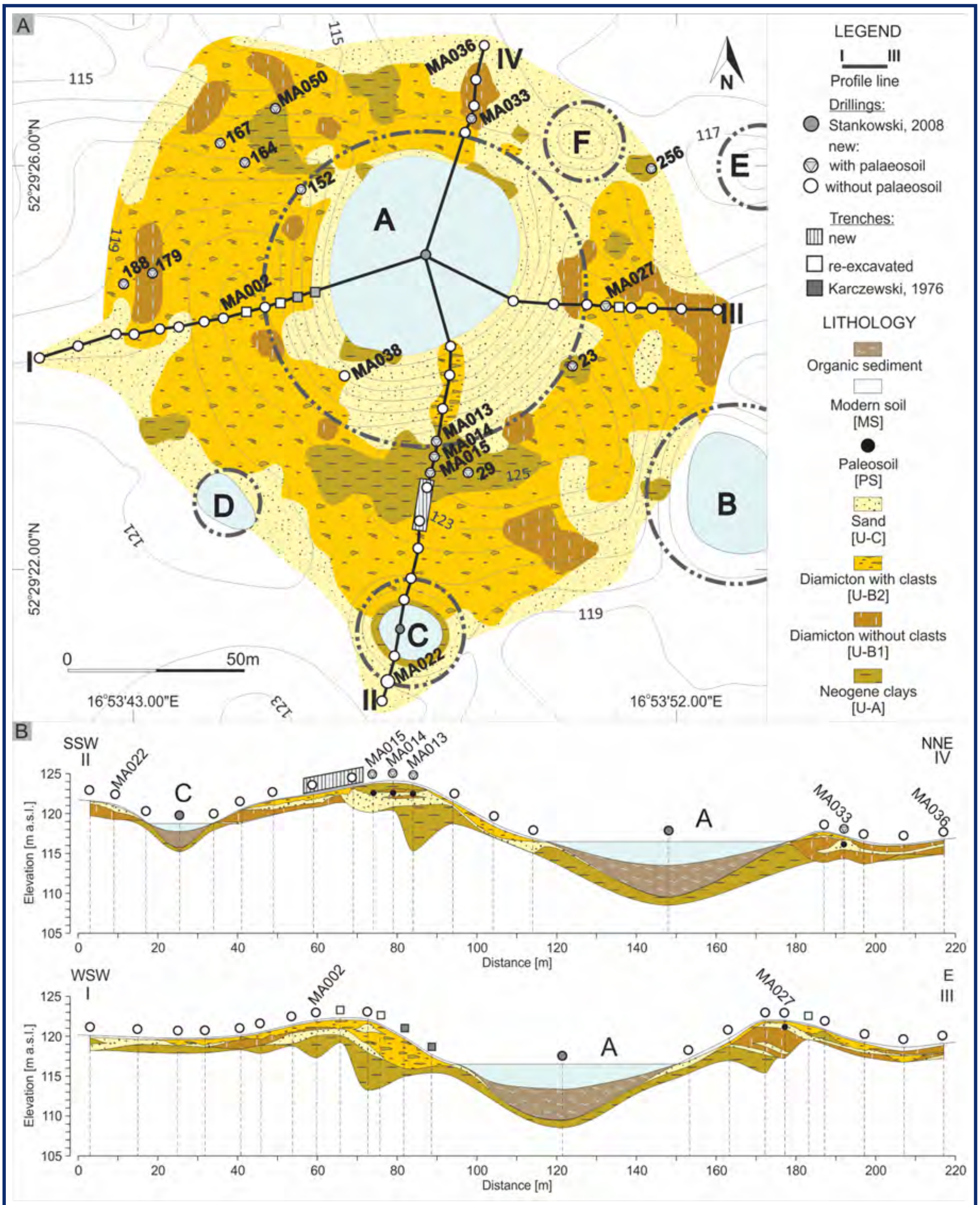

Figure 11. Spatial and vertical distribution of the major sediment types in the area of the biggest crater A. A) Surface sediment distribution (the modern soil is not included) based on over 100 sediment cores. B) Geological cross sections based on new data from Szokaluk et al. (2019), in addition to the previously documented trenches by Karczewski (1976) and sediment cores from Stankowski (2008). The cross sections are interpolated to the limit of existing data (drilling depth). In the figure, the locations of sediment cores and trenches used for generation of the cross sections, and the cores with documented paleosoil under ejecta layer are marked. (Figure after Szokaluk et al. (2019). Copyright: John Wiley and Sons – license number 4584750945787).

Figure 12. The lower part of thick ejecta layer, close to the crater rim, composed of Neogene clay and diamicton with Neogene clay clasts, overlying Pleistocene sand with developed thin palaeosoil. The age of the soil was ^{14}C dated to app. 5000–5500 cal. years BP (Szczuciński et al., 2016).

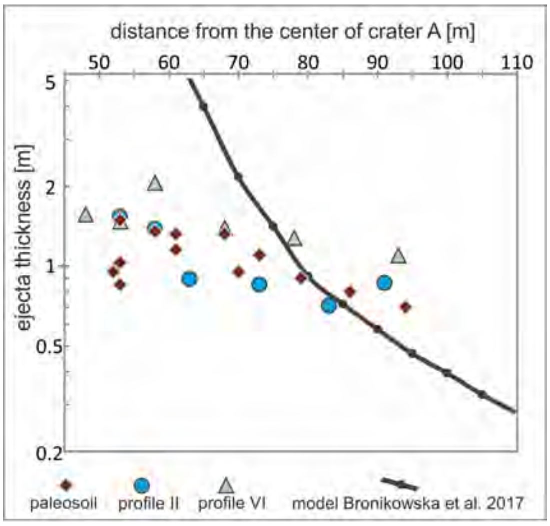

Figure 13. Change in ejecta blanket thickness with distance from the center of crater A, based on the thickness of diamicton with clasts interpreted as the ejecta layer in profile II and profile VI and the depth of the paleosoil horizon (various sites around the crater, see Figure 11A for locations). The modeled ejecta blanket thickness from the numerical model by Bronikowska et al. (2017) is provided for comparison. Note the logarithmic vertical scale. (Figure after Szokaluk et al. (2019). Copyright: John Wiley and Sons – license number 4584750945787).

made by a fragment approximately 3 m in diameter and moving at a speed of around 6 km/s. The numerical results provided relatively similar results to the geological evidence, for instance in case of ejecta deposits (**Figure 13**).

Did the event have any effect other than forming craters? Other well-known major impacts caused fires, powerful impact waves, earthquakes, tsunamis, and even climate change. The period of 5,000–5,500 years ago marks the beginning of the Neolithic in the Wielkopolska region, so naturally there are no historical descriptions of any effects. This means we need to rely on geological archives, such as sediments found in lakes (**Figure 14**, Pleskot et al. 2018). There are several post-glacial lakes near the craters which have accumulated sediments and plant and animal remains over thousands of years, making it possible to interpret environmental changes in the area, climate changes, results of human activity and local catastrophic events. Preliminary results indicate that the effects of the impact were far less significant than intuition suggests. Extensive fires were unlikely, and the range of the disaster was likely limited to the nearest surroundings of the actual impact sites (Pleskot et al. 2018), as suggested also by numerical models (Bronikowska et al. 2017).

This chapter is based on results of National Science Centre (Poland) grant No. 2013/09/B/ST10/01666.

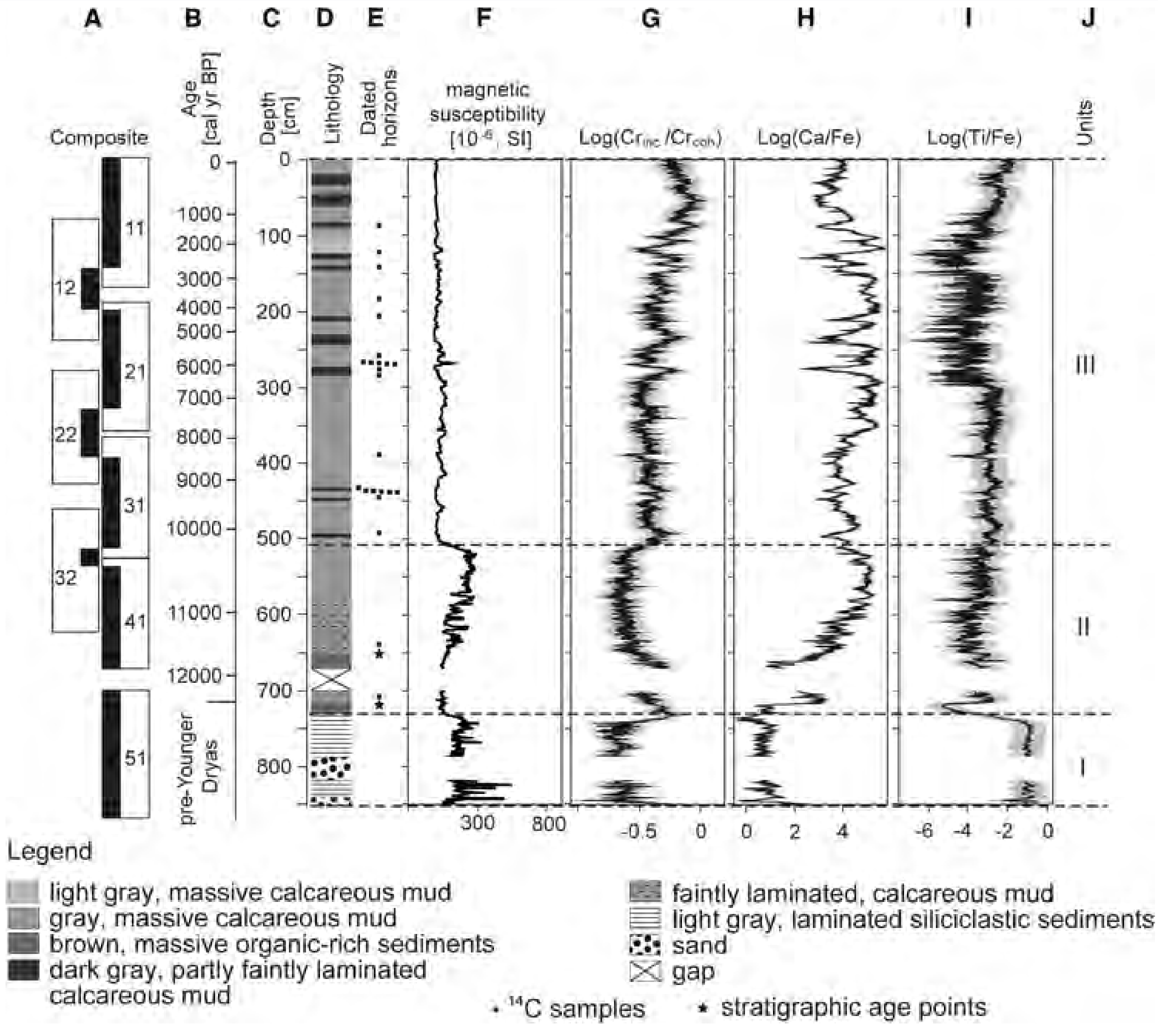

Figure 14. Sedimentology and geochemistry of sediment core from the central part of Strzeszyńskie Lake located app. 5 km away from the Morasko impact craters. The figure includes: a parts used from the twin cores for the core composite construction marked by black bars; b age scale based on the age-depth model; c sediment depth scale; d sediment lithology; e positions of samples for ^{14}C datings and horizons included in the age model; f magnetic susceptibility; g–i elemental ratios and properties revealed from XRF scanning. Shaded area indicates the 95% confidence level calculated from replicate measurements; j units determined on the basis of lithological and geochemical properties. Note the peak of magnetic susceptibility in the record around 5,500 cal. years BP. Figure after Pleskot et al. (2018).

Izabela Szuman-Kalita, Marek Ewertowski, Jakub Kalita, Leszek Kasprzak, Aleksandra Tomczyk

3. Site II: Skrzynki/Tomice – Inter-stream zone

3.1. Geological and geomorphological settings

Two sites near Tomice and Skrzynki are located at the foreland of the Poznań Phase (**Figure 1**) in the vicinity of the Buk–Mosina esker system, (see Rotnicki, 1960 for details). The first one is situated on glacial sands, whereas the Skrzynki is within an esker zone (**Figure 15, 16**). According to analysis of DEM and interpretation of the distribution of streamlined bedforms, these sites are situated within an inter-stream zone, between Września and Leszno ice streams in the area where MSGLs are absent (Map 1).

3.2. Sedimentological characteristics

Tomice

In Tomice, the sedimentary sequences start with the lower diamicton, then the glacifluvial sediments aged 180 ka (OSL, unpublished) is overlapped by the upper diamicton (Figure17A). Multiple sandy and silty intraclasts (e.g. **Figure 17D**) of varied lamination are found widespread within the glacifluvial sediments. Ewertowski (2009) described several relict frost-cracks within those glacifluvial sediments. Other permafrost features found within the outcrops are ice-wedge pseudomorph (**Figure 17C**) and load structures, disrupted ball-and-pillows, and load casts (**Figure 17E–F**). The

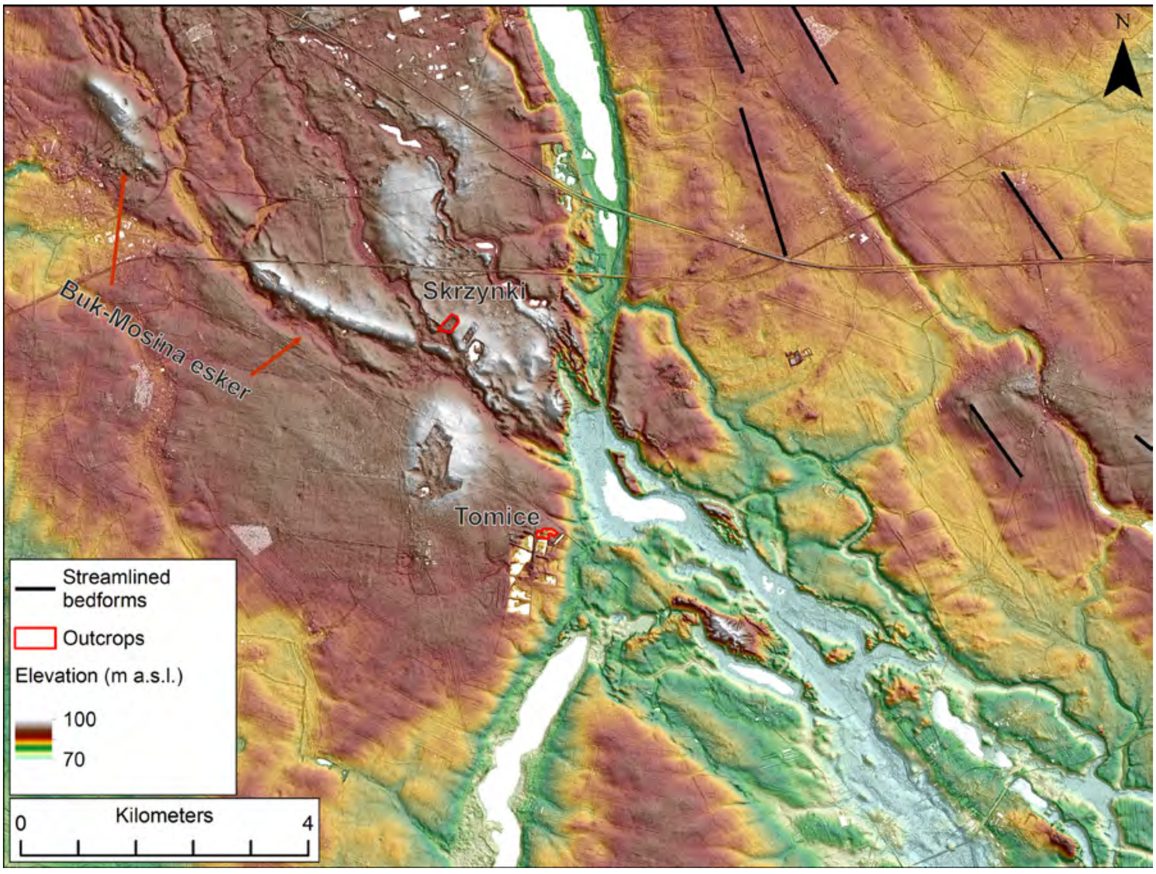

Figure 15. Location of the Tomice and Skrzynki sites.

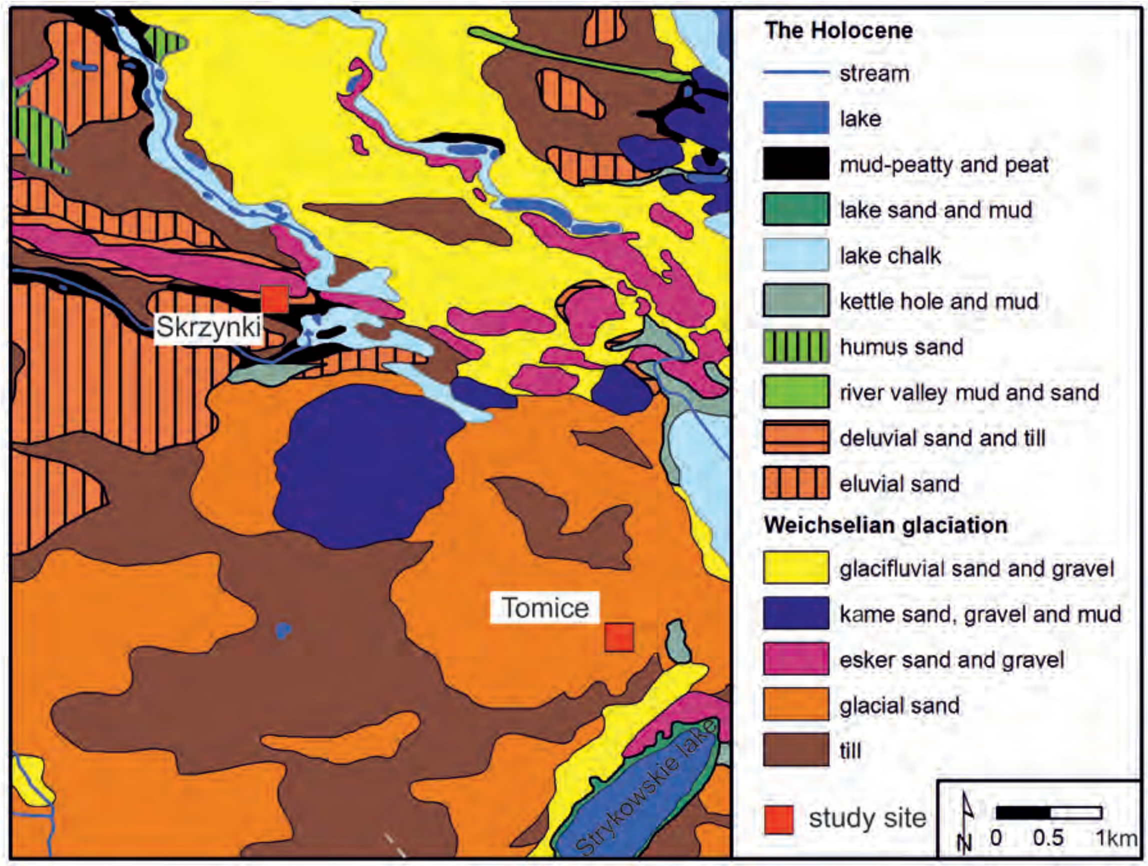

Figure 16. Geological map of Tomice and Skrzynki study sites, based on Chmal (1991, 1997), with some modifications.

Figure 17 (see next page). (A,B) The base of tectonically laminated diamicton. Continuous and discontinuous layers of sand and diamicton occur, albeit with contact that is well-defined. The laminae tend to incline from an angle of 40° (B) towards a horizontal position (A). Boudin structures can be found at the contact. Notice that (A) and (B) sections are distant by only c. 20 m. Traces of boudinage and sediment reworking are also clearly visible.

(C) ice-wedge pseudomorph directly beneath the diamicton horizon. It is c. 0.8 m long and 20–30 cm wide, filled with massive sand. At the top, the secondary wedge, filled with the diamicton, has developed (Photo: L. Szewczuk).

(D) Permafrost-related features in Tomice: silty sand intraclast with sharp edges and well-preserved primary lamination within cross-bedded sandy gravel sediments. It is c. 2 m wide and c. 0.4 m thick.

(E) Sheared load casts in Tomice: (A) till-on-till gradual contact, with sheared sandy casts below. The sandy bodies show little deformations along the edges, while the primary sedimentary lamination is well-preserved. The deformations occur within a c. 40 cm thick transition zone. The fine sand (the lightest one) is slightly deformed along the edges (some micro-faults). However, the primary sedimentary structure is generally well-preserved.

(F) Sheared silty sand load casts and disturbed thin sandy layers up to c. 0.6 m below the Weichselian diamicton. Beneath, there are quasi-horizontal disrupted layers of silty sand and sand which transit gradually into the non-deformed sand and silt below.

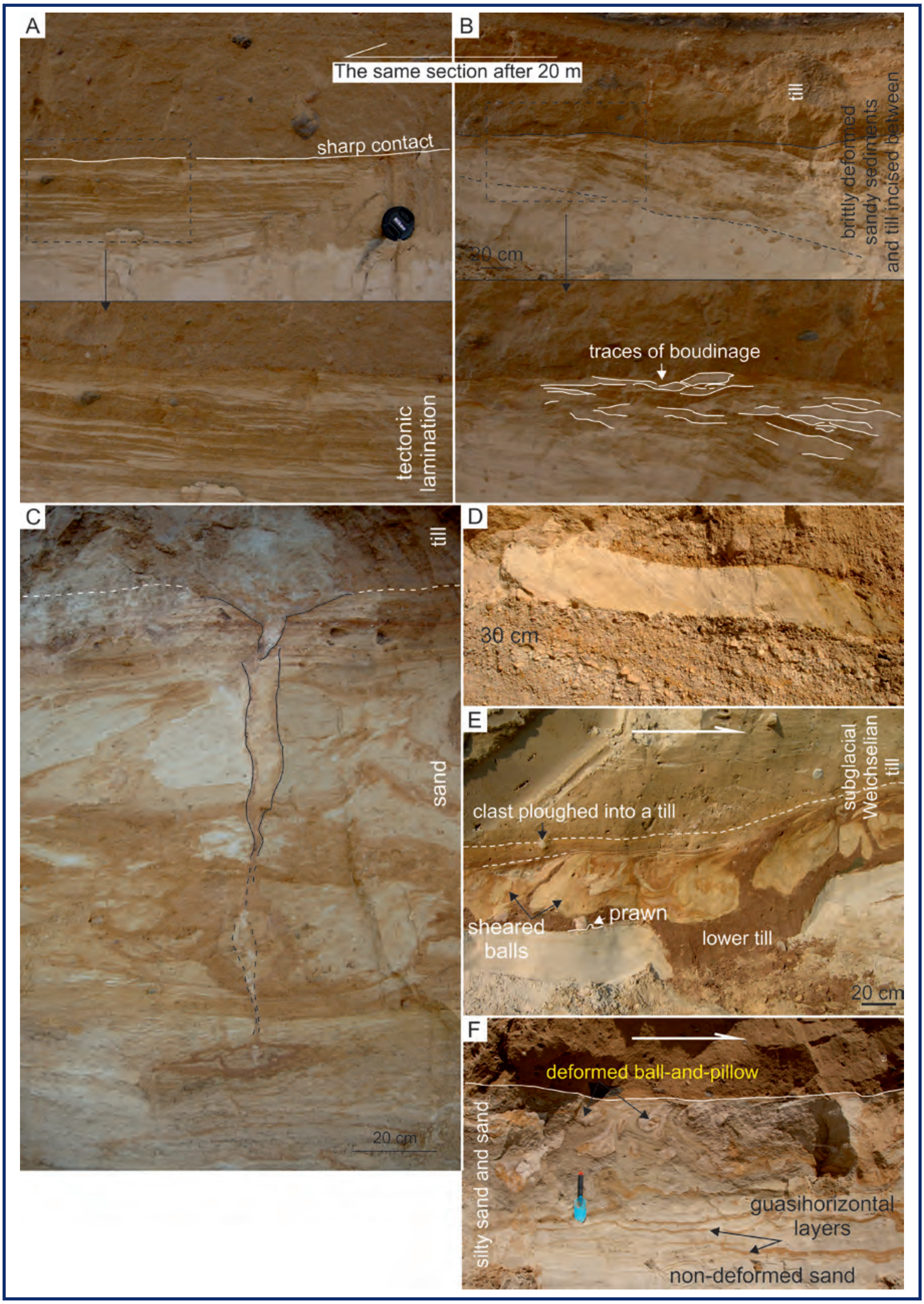

contact between diamicton and glacifluvial deposits is diversified, from sharp to gradual and deformational (**Figure 18**). The thickness of the deformed sediments beneath the Weichselian diamicton ranges from 0 (lack of deformations) to 2 m. The fine-grained substratum is locally heavily sheared (**Figure 18E**). A clastic dyke with burst-out structures within the thrust zone is shown in **Figure 19**. The displacement along the fault plane amounts to c. 1.0 m.

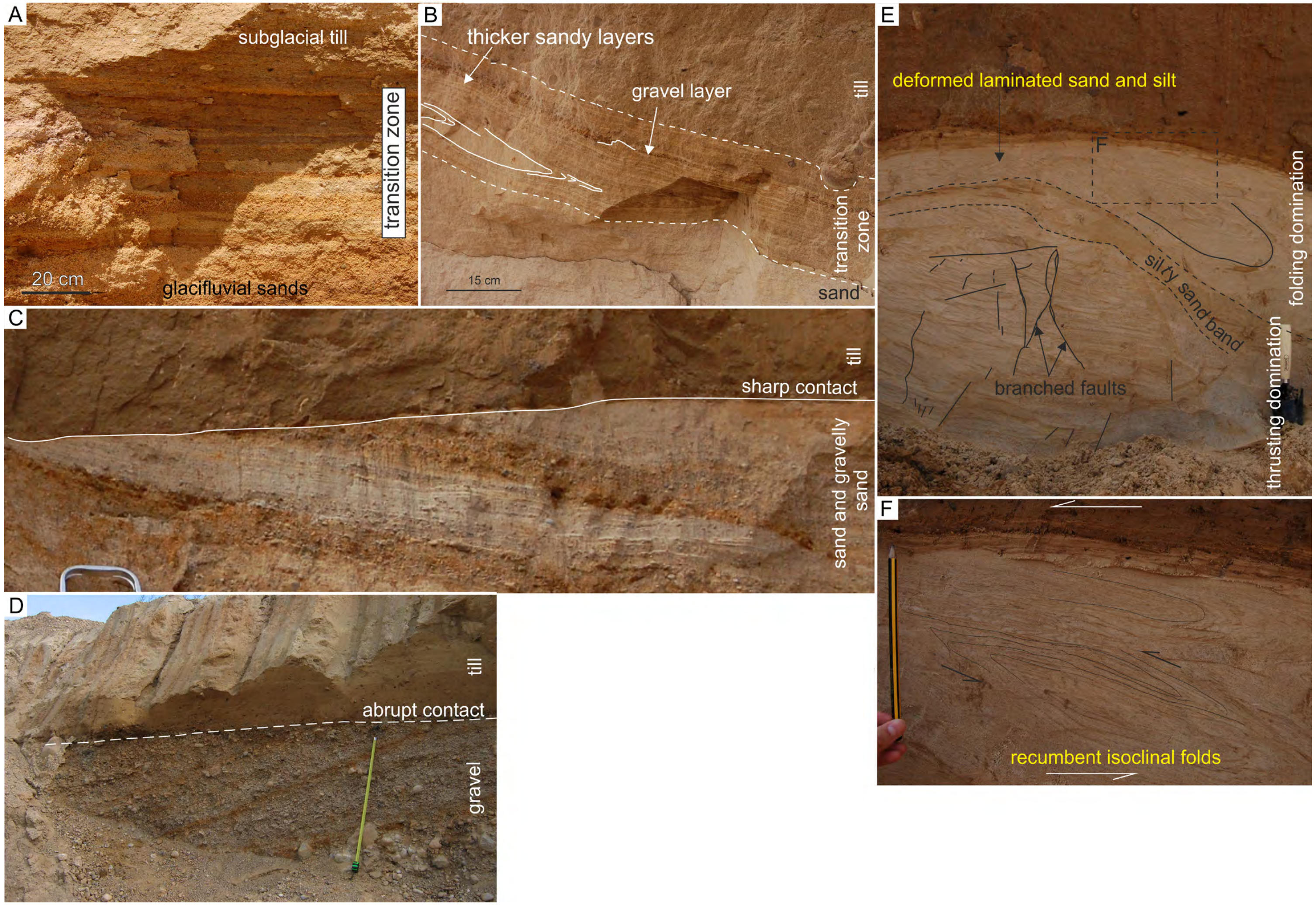

Figure 18. Contact between diamicton and glacifluvial sediments:
(A) stratification at the transition zone with visible plastering of diamicton and sand developed over coarse-grained sands and gravels. Notice that mixing does not occur.
(B) tectonic layering: alternating laminae of diamicton and sand and sheared recumbent fold.
(C) sharp contact between diamicton and cross-bedded gravels without any visible mixing at the contact. There is also a lack of deformation in the substratum.
(D) sharp contact between diamicton and gravels. Mixing is restricted to up to 10 cm and wherever any deformations of cross-bedded gravels occur.
(E) sheared sands in more ductile (upper) and brittle (lower) style. Brittle deformations reveal conjugated sets of micro-shears/faults, but the fault planes are not straight; they are branching. (F) recumbent isoclinal folds. Beneath this deformed zone, c. 1 m below the diamicton fine-grained and laminated (not deformed) sand occurs.

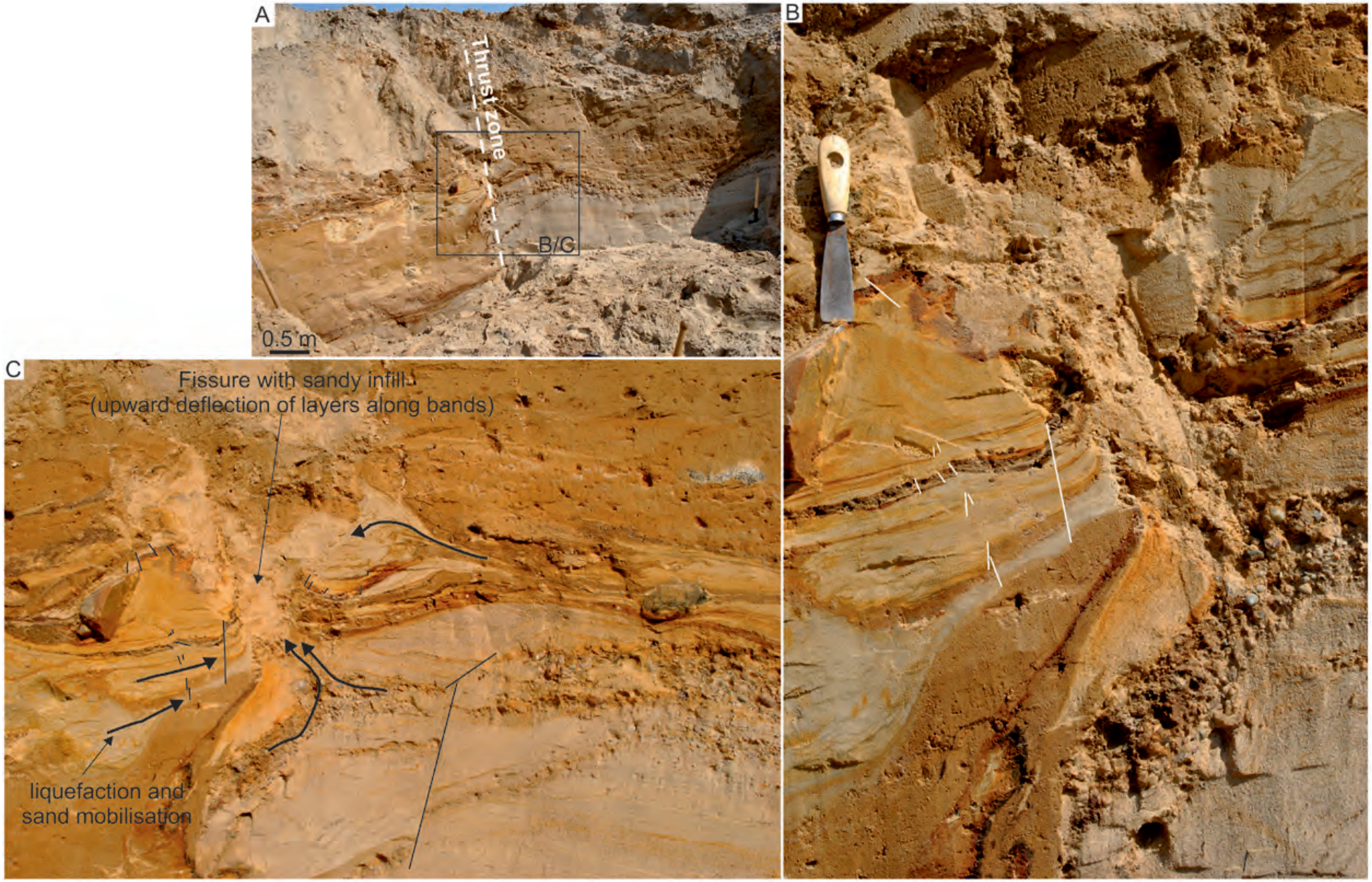

Figure 19. (A) Hydrofracture developed along thrust plane; (B) The fracture is filled with sand and gravels, suggesting high pore-water pressure. Along the edges of these cracks, interrupted layers show upward deflection, concordant with the direction of the water flow, marked with black curved arrows; (C) Notice that the sediments just beneath the hydrofracture are deformed brittly, indicating that the substratum was rigid, probably frozen.

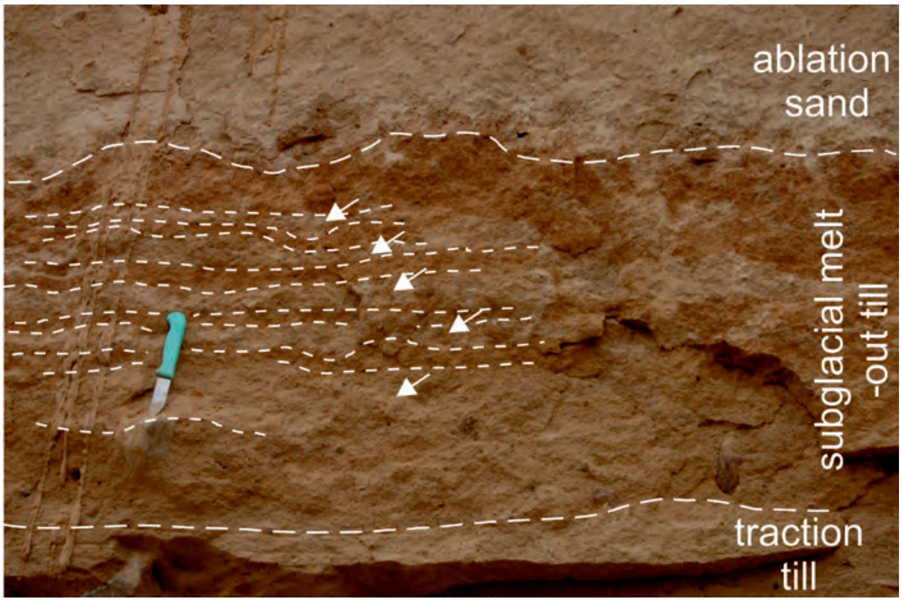

Figure 20. Subglacial melt-out till. Notice the lighter (sand-rich, marked with white arrows) and reddish (rich finer particles) layers; they are disturbed and locally discontinuous but still clearly visible.

The thickness of the Weichselian diamicton layer ranges from 0.8 to 2 m. Structural and colour differences within this unit allow for dividing the whole diamicton layer into two parts. The lower one (generally massive, c. 0.6–1.2 m thick) with single stringers of sand (see **Figure 20**) transits gradually into the upper part, c. 0.4–0.6 cm thick. This upper part of the diamicton is quasi-banded, consisting of lighter more sandy layers and darker finer ones, enhanced by a reddish-brown colour. The layers are occasionally distorted and interrupted, and their thickness changes from 2 cm to 10 cm. The vertical variability of fabric orientation within the massive diamicton is low. The deviation from the mean direction – 224.75 (V1 eigenvector) — is only 9.5º. Eigenvalues in Tomice show 'high' to 'very high' values – S1 between 0.87 and 0.95; cf. (Thomason and Iverson, 2006).

Skrzynki Site

The section in Skrzynki (**Figure 21**) shows deformed sandy deposits, truncated by the diamicton (most of the diamicton horizon was excavated) of up to 2 m thick. The clast fabric shows V1 equalling 209 and moderate eigenvalue (S1 – 0.69). The glacifluvial sands reach a depth of at least 2.5 m. They are folded, faulted, thrusted and brittle-sheared with oversteepenings of up to 90°.

3.3. Depositional model

Two contrasting models can explain the formation and deformation of subglacial sediments. The first assumes that subglacial deformations are pervasive, thereby requiring a thick deformation bed and high strains (Boulton and Jones, 1979; Alley, 1990; Kamb, 1991; van der Meer et al., 2003; Menzies et al., 2006). In contrast, Piotrowski and Kraus (1997) concluded that pervasive deformation did not occur beneath the Weichselian ice sheet in north-western Germany. This second model argues that a glacial bed constitutes a 'mosaic' composed of deforming and non-deforming patches that transit in time and space (Piotrowski and Kraus, 1997). Variability at the ice/bed interface develops mainly in response to hydrological conditions (Hoffmann and Piotrowski, 2001; Piotrowski et al., 2004) and lithology, though mainly with regard to the thermal regime. An additional factor influencing the glacier's bed rheology was most likely related to the occurrence of subglacial permafrost. Cutler et al. (2000) suggest that the ice/permafrost interactions were probably more significant beneath the former ice sheets than had been previously proposed. The properties of sediments at temperatures around the pressure melting point greatly depend on the grain-size distribution and water/ice content within the sediment. The interpretation of sedimentary structures in terms

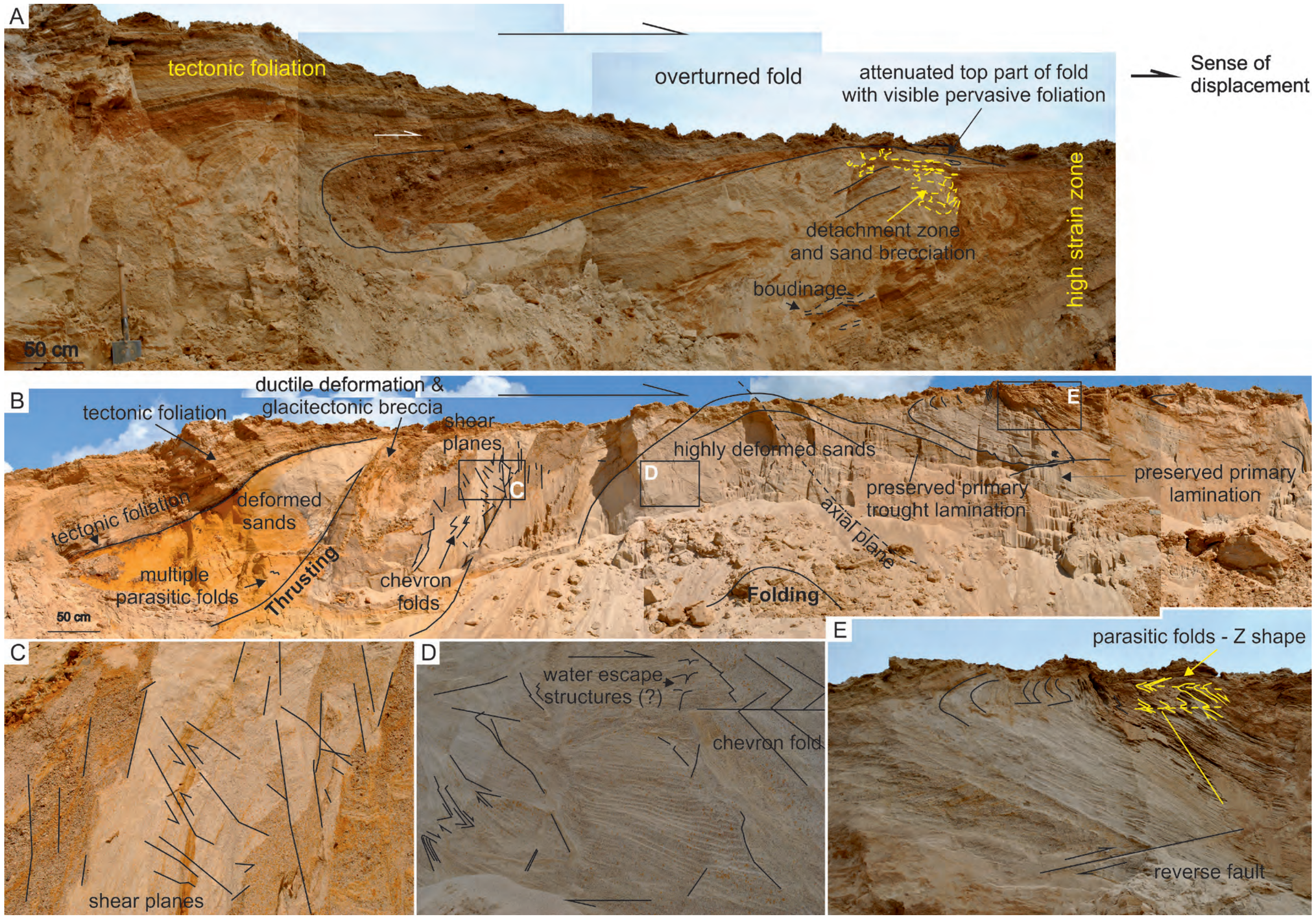

Figure 21. Mesoscale folding, thrusting and faulting of gravelly sand deposits in the Skrzynki site. Notice that the diamicton layer, c. 2 m thick, was removed during mining activities: (A) thigh inter-limb overturned fold with traces of boudinage with brecciation and detachments. Tectonic foliation occurs close to the contact. A general strike of approximately northwest to southeast, perpendicular to the MSGLs' orientation in Wielkopolska; (B) a large-scale thrusted and folded sequence of sands and gravelly sand, with an open inter-limb angled asymmetrical fold in the centre; (C) faulted gravelly sand with multiple shear planes, oversteepening of up to 90°; (D) faulted and folded sand with single downwarped and broken laminae (possibly water-escape structures), presence of thrusts and chevron folds; (E) faulted and partly deformed fold's limb. Notice that the primary sedimentary structure is also clearly visible.

of identifying the subglacial thermal regime, i.e. whether deformation occurred at temperatures above or below the pressure melting point, is problematic (Hart and Boulton, 1991; Waller et al., 2009; Hambrey and Glasser, 2012; Szuman et al., 2013).

The depth of deformations in the studied outcrops greatly varied — from a sharp erosional contact and a deformation layer of a few centimetres thick to even up to c. 2 metres. The sharp erosional contact between the homogeneous tills and undeformed sediments underneath contrasts with the deforming bed model which assumes the glaciotectonic deformations of the substratum. But the areas where the deformations occur remain consistent. However, the typical depth of the deformations found in the Tomice area is smaller than the predicted deformation depth according to the deforming bed concept. Also, the strains are low because the sandy casts are only slightly skewed while other deformational structures are easily recognisable; the sediments are not homogenised. The massive diamicton is interpreted as a traction till, and the banded one as a subglacial melt-out till. Even though the traction till is massive, single sand stringers were observed. According to the approach proposed by Hooyer and Iverson (2000), the S1 values between 0.87 and 0.95 denote a strain of between c. 10 and 40. The preservation of sandy stringers repudiates the concept of pervasive strains within the deforming bed. Thus, it is suggested that basal sliding, rather than bed deformation, was the main movement mechanism of the ice sheet over the Tomice site. Sliding was supported by the high water pressure beneath the ice which arose within a thin thawing layer that developed between the ice sole and the rigid, permafrozen substratum.

The ice sheet in the Tomice study site overrode and deformed the top part of the glacifluvial deposits. However, the depth and style of deformation are swiftly changeable in space. The variabilities in sedimentary structures confirm the co-occurrence of frozen dry and wet mobile spots in kilometre-, metre- and even a dozen centimetre-scales. The ice-wedge pseudomorph, with subglacial till on top, indicates that: (1) there was permafrost; and (2) that the till was deposited on it. The ductile style of deformation (i.e. load casts and hydro-fracture) indicates a high subglacial pore-water pressure, even if the sandy substratum has a high drainage capacity. The nature of deformations in Tomice, indicating a high water content and pressure, suggests the occurrence fast-flowing ice. However, the deformations in the Skrzynki site do not support the fast ice-flow model. These kinds of structures are typical of slower compressive ice flow, (cf. Hart and Boulton, 1991), and are also typical of proglacial deformations. They may be linked then to the phase of non-pervasive, localised deformation *sensu* Jørgensen and Piotrowski (2003). When pore-water pressure rose, the ice sheet sped up and overrode the proglacially deformed sediments, ‘beheading’ its top part (like the truncated and attenuated fold in **Figure 21**).

Because the shear stresses operating on the substratum are not identical in all points/regions, especially on account of the changeable hydrological conditions that arise (i.e. from changes in the sediments grain-size distribution), the mosaic pattern of deformations is common. Some patches were ‘wet’ and mobile in favour of ice flow speeding up, while others were ‘frozen’, rigid, and coupled with the ice sole. The second type of patches slowed the ice flow and caused a compressive ice flow, mesoscale glacitectonic deformations, and sharp contacts. This is consistent with the sticky-spots model (Alley, 1993; Stokes et al., 2007) or the mosaic bed conception (Piotrowski and Kraus, 1997; Jørgensen and Piotrowski, 2003; Piotrowski et al., 2004; Piotrowski et al., 2006).

Additionally, taking geomorphology into account, the relief of the study area is slightly different from neighbouring areas. The MSGLs are well-developed on the western and eastern sides of the Tomice–Skrzynki area, suggesting that the fast ice stream flowed over the wet and warm substratum. The lack of MSGLs within the Tomice–Skrzynki area and the occurrence of permafrost-related features — i.e. (i) mesoscale glacitectonic, (ii) ice-cracks (Ewertowski, 2009), (iii) ice wedge pseudomorph and intraclasts within the glacifluvial unit, (iv) erosional contacts, (v) brecciation and tectonic lamination, (vi) thaliks-marks, (vi) load structures similar to those described from Siberia — all suggest that the ice flow was slower in this region (Szuman et al. 2013) when compared to the MSGLs-rich regions. Both sedimentological and geomorphological evidences suggest that this area was in the former inter-stream zone, implying the potential development of lateral shear moraines and associated deformations.

This chapter is based on results of National Science Centre (Poland) grant No. 2015/17/D/ST10/01975.

Izabela Szuman-Kalita, Marek Ewertowski, Jakub Kalita, Leszek Kasprzak, Aleksandra Tomczyk

4. Site III: Kuślin – Ice marginal deformations

4.1. Geological and geomorphological setting

According to the geological map by Pluczyński and Sydow (1993), the Kuślin site is located at the border between an outwash plain and till plain at the east side of the Lwówek–Rakoniewice rampart. On LiDAR DEM, there is also a clearly visible crest, located to the east of the rampart. As to the geological maps (Pluczyński and Sydow, 1993; Michalska and Winnicki, 2003), this crest comprises of frontal moraines, eskers, thrust moraines, kames, and structural crevasse infill ridges. Beginning to the east of the Lwówek–Rakoniewice rampart is a streamlined bedform flow-set belonging to the Leszno palaeo-ice stream (**Figure 22**).

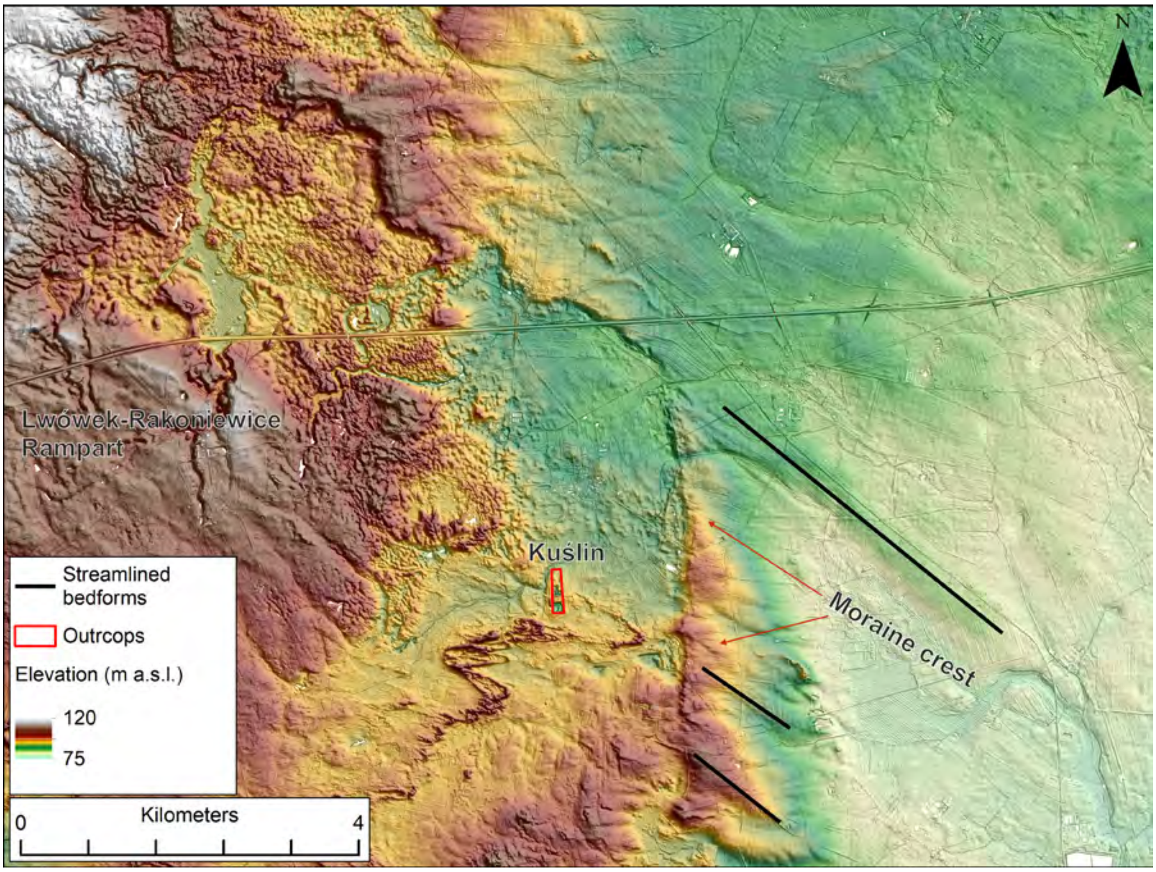

Figure 22. Location of the Kuślin site.

4.2. Sediments' description

The exposed sections are c. 250 m long and up to 7 m high, with varied orientations. A wide variety of glacitectonic and permafrost features were found in this site. The bottom part of the sedimentary sequence is composed of highly deformed sands, gravels, silts, and diamicton (**Figures 23–25**). The top of deformations is either excavated or overlaid by silt deposits (**Figure 24A**), massive sand (**Figure 24B**) or a banded diamicton that gradually transits into massive sand (**Figure 24C**). Several clastic dykes were identified along certain sections (**Figures 23, 24C,D, 25A**). Sands and gravels

Figure 23. Highly folded glacifluvial sediments. Notice the subglacial till block to the right with preserved sandy inclusions. A hydrofracture had developed between the deformed lithofacies.

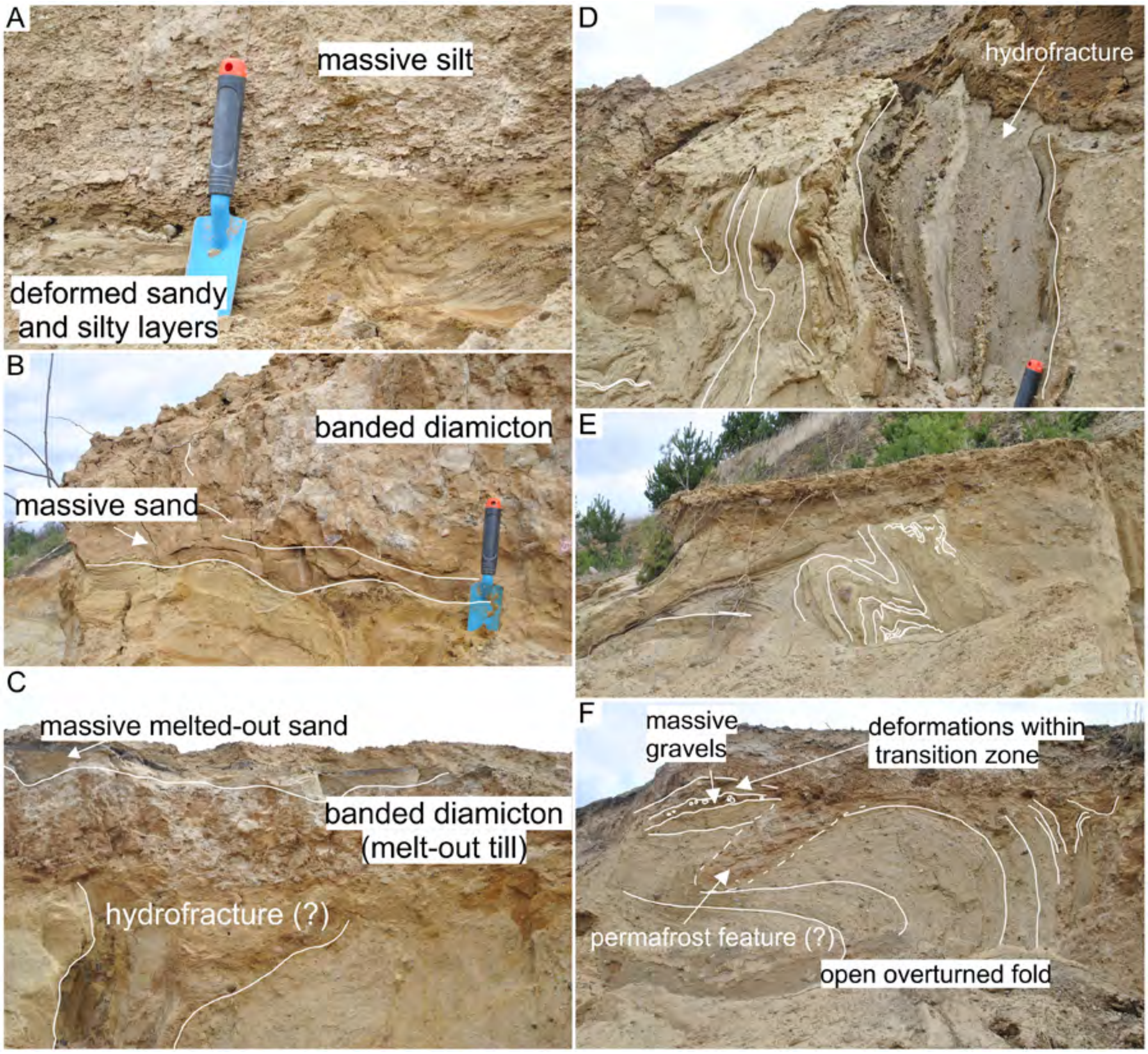

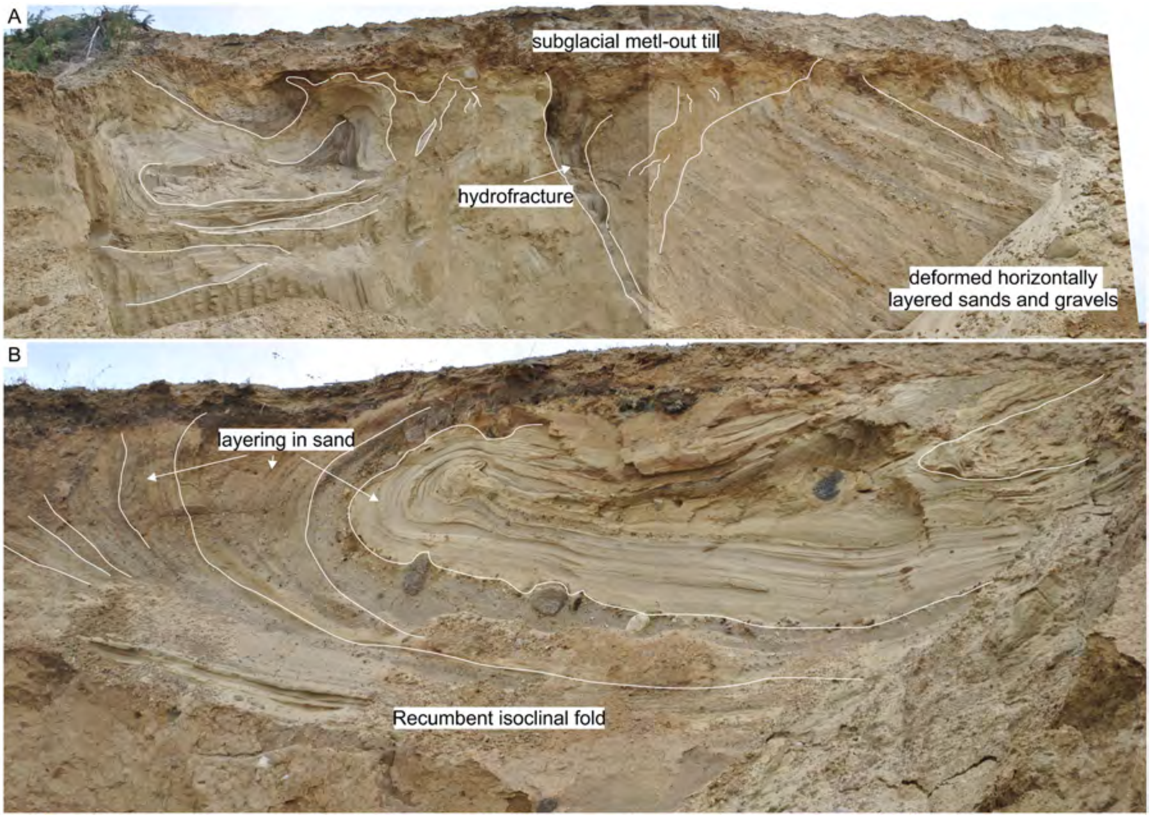

Figure 25. (A) Ductile deformations (to the left) and brittle one to the right – block of normally graded glacifluvial sands and gravels with well-preserved layering. A hydrofracture developed between deformed units. The top of deformed sediments is covered by subglacial melt-out till. (B) Recumbent isoclinals fold with undisturbed sandy layering within it.

were injected under high pore-water pressure into veins formed between deformed lithofacies. The surrounded sediments are intensively deformed (**Figure 24D**). The section revealed also series of deformation structures, mostly different types of folds (**Figures 23, 24E,F, 25B**), blocks of deformed subglacial (Weichselian?) till (**Figure 23**), and glacifluvial sediments with preserved horizontal lamination (**Figure 25A**).

Figure 24 (see previous page). (A) Massive silty deposits on top of deformed sandy gravels; (B) gradual contact between deformed sands and silty sediments on it. Multiple ductile deformations are visible within the transition zone. (B) Massive sand (probably melted from the ice) on top of the deformed sands (C) Banded, sandy diamicton on top of the deformed sand. Massive sand is deposited on top. (D) A hydrofracture filled with sand and gravels, suggesting high pore-water pressure. The surrounding sediments are highly defored (ductille deformations). (E) Overturned folds, developed within layers with low strength contrast (F) An open overturned fold with preserved continuity of sandy layers. Notice the wedge-like structure (possible deformed therml-contraction-crak pseudomorph) cross-cutting the fold, but with orientation almost parallel to the fold axes, meaning that this feature had developed before the deformation event.

4.3. Interpretation

The deformations in the Kuślin site can be related to older glaciations or were caused by the local re-advancing of the local ice margin in subglacial permafrozen conditions. The Kuślin site is only c. 1.5 km away from the local marginal moraines, thus cold-based ice is highly probable in such a location. However, the scale of deformations is quite large, which might suggest that some components had been associated with older structures.

We did not find any subglacial till on top of the deformed sediments, which might suggest that the whole sequence was not so much overridden by an ice sheet as being formed in a proglacial/ submarginal position. This interpretation may be bolstered by the diamicton raft (probably subglacial Weichselian till) found at the lower part of the deformed sequence. While the investigation is still ongoing, our current interpretation is that Leszno ice stream retreat was interrupted by a period of dynamic equilibrium in the local ice margin. Small oscillations have caused the production of minor pushed moraines on the northern side of the Lwówek–Rakoniewice rampart and along the morainic crest (see the geological maps by Pluczyński and Sydow, 1993). The location of the Kuślin site within the former submarginal position (c. 1.5 km from the inferred ice margin) implies favourable conditions for large-scale folding and thrusting. Subglacial meltwater was trapped between the frozen cold-based ice snout (indicated by marginal moraines) east of the Kuślin site and elevation of the Lwówek–Rakoniewice rampart west of Kuślin. Water was trapped but escaped with high pressure between deformed units during bed deformation. Highly pressurised water can also cause ice fragmentation. The thawing ice covered the unit of deformed sediments by melt-out deposits: the localised silty kame deposits, subglacial sandy, and banded melt-out till or massive sand melted from the ice. To the north and north east of Kuślin, the landscape is more closely associated with the degradation of former belt of debris-covered snout and thus represents a chaotic hummocky topography. Sedimentological analyses to verify these hypotheses are ongoing.

This chapter is based on results of National Science Centre (Poland) grant No. 2015/17/D/ST10/01975.

Acknowledgements

We would to thank Dean of the Faculty of Geographical and Geological Sciences, Adam Mickiewicz University for financial and organizational support. This work was supported by Polish National Science Centre (NCN) grant numbers:

- 2015/17/D/ST10/01975
- 2013/09/B/ST10/01666

References

Abdulmalik, O., 2015. Global Atlas for Renewable Energy-Geothermal Component, Proceedings World Geothermal Congress 2015.

Alley, R.B., 1990. Multiple steady states in ice-water-till systems. Ann Glaciol, 14, 1–5.

Alley, R.B., 1993. In search of ice-stream sticky spots. J Glaciol, 39(133).

Augustowski, B., 1956. Spostrzeżenia ze strefy kontaktowej zlodowacenia bałtyckiego i środkowopolskiego w okolicy Wschowy. Badania Fizjograficzne nad Polską Zachodnią, 3, 113–123.

Boulton, G., Jones, A., 1979. Stability of temperate ice caps and ice sheets resting on beds of deformable sediment. J Glaciol, 24(90), 29–43.

Boulton, G.S., Dongelmans, P., Punkari, M., Broadgate, M., 2001. Palaeoglaciology of an ice sheet through a glacial cycle:-the European ice sheet through the Weichselian. Quaternary Sci Rev, 20(4), 591–626.

Bronikowska, M., Artemieva, N.A., Wünnemann, K., 2017. Reconstruction of the Morasko meteoroid impact—Insight from numerical modeling. Meteorit Planet Sci, 52(8), 1704–1721. 10.1111/maps.12882

Cepek, A.G., 1965. Geologische Ergebnisse der ersten Radiokarbondatierungen von Interstadialen im Lausitzer Urstromtal. Geologie, 14(5–6), 617–642.

Chmal, R., 1990. Detailed geological map of Poland at scale 1:50 000. Poznań Sheet. PIG–PIB, Warsaw.

Chmal, R., 1991. Szczegółowa Mapa Geologiczna Polski. Arkusz Stęszew. PIG, Warszawa.

Chmal, R., 1997. Objaśnienia do Szczegółowej mapy geologicznej Polski, 1: 50000, ark. Stęszew. Państwowy Instytu Geologiczny, Warszawa.

Cutler, P.M., MacAyeal, D.R., Mickelson, D.M., Parizek, B.R., Colgan, P.M., 2000. A numerical investigation of ice-lobepermafrost interaction around the southern Laurentide ice sheet. J Glaciol, 46(153), 311–325.

Czerwonka, J.A., 2004. Śląska i wielkopolska prowincja litostratygraficzna glin zwałowych. Prz. Geol, 52(5), 421–429.

Czerwonka, J.A., Krzyszkowski, D., 1994. Pleistocene stratigraphy and till petrography of the central Great Poland Lowland, western Poland. Folia Quaternaria, 65, 7–71.

Database, E.I., 2019. http://www.passc.net/EarthImpactDatabase/index.html.

Ewertowski, M., 2009. Ice-wedge Pseudomorphs and Frost-cracking Structures in Weichselian Sediments, Central-West Poland. Permafrost and Periglacial Processes, 20(4), 316–330. 10.1002/ppp.657

Ewertowski, M.W., Kijowski, A., Szuman, I., Tomczyk, A.M., Kasprzak, L., 2017. Low-altitude remote sensing and GIS-based analysis of cropmarks: classification of past thermal-contraction-crack polygons in central western Poland. Geomorphology, 293, 418–432. 10.1016/j.geomorph.2016.07.022

Górska, M., 1995. Właściwości i cechy diagnostyczne bazalnych glin morenowych vistulianu jako wyraz dynamiki środowiska depozycyjnego ostatniego lądolodu na Nizinie Wielkopolskiej. Bad. Fizjograf. nad Polską Zach., Ser. A, Geogr. Fiz, 46, 29–62.

Górska, M., 2000. Wybrane właściwości petrograficzne vistuliańskich moren dennych środkowej i zachodniej Wielkopolski oraz ich znaczenie dla oceny dynamiki ostatniego lądolodu, 28. Wydawnictwo poznańjkiego towarzystwa przyjaciół nauk.

Hambrey, M.J., Glasser, N.F., 2012. Discriminating glacier thermal and dynamic regimes in the sedimentary record. Sediment Geol.

Hart, J.K., Boulton, G.S., 1991. The interrelation of glaciotectonic and glaciodepositional processes within the glacial environment. Quaternary Sci Rev, 10(4), 335–350.

Heine, K., Reuther, A.U., Thieke, H.U., Schulz, R., Schlaak, N., Kubik, P.W., 2009. Timing of Weichselian ice marginal positions in Brandenburg (northeastern Germany) using cosmogenic in situ (10)Be. Z Geomorphol, 53(4), 433–454. Doi 10.1127/0372-8854/2009/0053-0433

Hermanowski, P., Piotrowski, J.A., Szuman, I., 2019. An erosional origin for drumlins of NW Poland. Earth Surf Proc Land, in press. 10.1002/esp.4630

Hoffmann, K., Piotrowski, J., 2001. Till melange at Amsdorf, central Germany: sediment erosion, transport and deposition in a complex, soft-bedded subglacial system. Sediment Geol, 140(3–4), 215–234.

Hooyer, T.S., Iverson, N.R., 2000. Clast-fabric development in a shearing granular material: Implications for subglacial till and fault gouge. Geol Soc Am Bull, 112(5), 683–692.

Jørgensen, F., Piotrowski, J.A., 2003. Signature of the Baltic ice stream on Funen Island, Denmark during the Weichselian glaciation. Boreas, 32(1), 242–255.

Kamb, B., 1991. Rheological nonlinearity and flow instability in the deforming bed mechanism of ice stream motion. Journal of Geophysical Research, 96(B10), 16585–16516,16595.

Karczewski, A., 1976. Morphology and lithology of closed depression area located on the northern slope of Morasko Hill near Poznań. In: H. Hurnik (Ed.), Meteorite Morasko and the Region of Its Fall. Seria Astronomia. Adam Mickiewicz University Press, Poznań, pp. 7–20.

Karwowski, Ł., Kusz, J., Muszyński, A., Kryza, R., Sitarz, M., Galuskin, E.V., 2015. Moraskoite, Na2Mg (PO4) F, a new mineral from the Morasko IAB-MG iron meteorite (Poland). Mineral Mag, 79(2), 387–398.

Karwowski, Ł., Kryza, R., Muszyński, A., Kusz, J., Helios, K., Drożdżewski, P., Galuskin, E.V., 2016. Czochralskiite, Na4Ca3Mg (PO4) 4, a second new mineral from the Morasko IAB-MG iron meteorite (Poland). European Journal of Mineralogy, 28(5), 969–977.

Kasprzak, L., 2003. Model sedymentacji lądolodu vistuliańskiego na Nizinie Wielkopolskiej. Wydawnictwo Naukowe UAM, Poznan.

Kasprzak, L., Kozarski, S., 1991. Stosunek rzeźby strefy marginalnej fazy leszczyńskiej ostatniego zlodowacenia do podłoża previstulianskiego w południowo-zachodniej Wielkopolsce. Badania Fizjograficzne nad Polską Zachodnią, 42, 85–101.

Kozarski, S., 1986. Time scales and the rhythm of Vistulian geomorphic events in the Polish Lowland. Czasopismo Geograficzne, 57(2), 247–270.

Kozarski, S., 1991. Litostratygrafia górnego plenivistulianu Niziny Wielkopolskiej w granicach ostatniego zlodowacenia: nowe dane i interpretacje [Lithostratigraphy of the upper Plenivistulian in the Wielkopolska Lowland during the last glaciation: new data and interpretations]. In: A. Kostrzewski (Ed.), Geneza, litologia i stratygrafia utworów czwartorzędowych [Genesis, lithology and stratigraphy of Quaternary sediments]. Geografia, pp. 471–496.

Kozarski, S., 1992. Lithostratigraphy of upper Plenivistulian deposits in the Great Poland Lowland within the area of the last glaciation. SGU series Ca. Research paper(81), 157–162.

Kozarski, S., 1995a. Deglaciation of Northwestern Poland: environmental conditions and geosystem transformation (~20 ka – 10 ka BP). Dokumentacja Geograficzna IGiPZ PAN, 1.

Kozarski, S., 1995b. The periglacial impact on the deglaciated area of northern Poland after 20 kyr BP. Biuletyn Peryglacjalny, 34, 73–102.

Krygowski, B., 1952. The issue of the Quaternary and the substrata of the central part of the Great Poland Lowland. Biuletyn Państwowego Instytutu Geologicznego, 66, 189–217.

Krygowski, B., 1961. Geografia fizyczna Niziny Wielkopolskiej: Geomorfologia. Państwowe Wydawnictwo Naukowe, Poznań.

Krygowski, B., 1967. Ważniejsze problemy plejstocenu Polski Zachodniej. In: R. Galon, J. Dylik (Eds.), Czwartorzęd Polski. Państwowe Wydawnictwo Naukowe, Warszawa. PWN, Warszawa, pp. 167–205.

Krygowski, B., 1972. Nizina Wielkopolska, Geomorfologia Polski, pp. 186–223.

Krygowski, B., 1975. Niektóre problemy z morfodynamiki Niziny Wielkopolskiej. Badania Fizjograficzne nad Polską Zachodnią, 27, 89–156.

Krzyszkowski, D., Gratzke, B., 1994. History of glaciation in the zone of maximum extent of the Late Weichselian ice-sheet near Leszno, western Poland. Folia Quaternaria, 65, 143–193.

LIAG, 2015. Karten des Temperaturfeldes im Untergrund Deutschlands in 2000 m. Institut für Angewandte Geophysik, Leibniz.

Liszkowski, J., 1987. Zonal arrangement of thermal regimes of Pleistocene ice sheets as indicated by field data from Poland, The Physical Basis of Ice Sheet Modelling (Proceedings of the Vancouver Symposium, pp. 121–130.

Luthgens, C., Bose, M., Preusser, F., 2011. Age of the Pomeranian ice-marginal position in northeastern Germany determined by Optically Stimulated Luminescence (OSL) dating of glaciofluvial sediments. Boreas, 40(4), 598–615. DOI 10.1111/j.1502-3885.2011.00211.x

Lüthgens, C., Böse, M., Krbetschek, M., 2010. On the age of the young morainic morphology in the area ascribed to the maximum extent of the Weichselian glaciation in north-eastern Germany. Quaternary International, 222(1–2), 72–79.

Marks, L., 2002. Last glacial maximum in Poland. Quaternary Sci Rev, 21(1–3), 103–110.

Marks, L., 2010. Timing of the Late Vistulian (Weichselian) glacial phases in Poland. Quaternary Sci Rev, 81–88.

Marks, L., 2012. Timing of the Late Vistulian (Weichselian) glacial phases in Poland. Quaternary Sci Rev, 44, 81–88.

Menzies, J., van der Meer, J.J., Rose, J., 2006. Till—as a glacial “tectomict”, its internal architecture, and the development of a “typing” method for till differentiation. Geomorphology, 75(1–2), 172–200.

Michalska, D., Winnicki, J., 2003. Szczegółowa Mapa Geologiczna Polski. Arkusz Grodzisk. PIG, Warszawa.

Muszyński, A., Kryza, R., Karwowski, Ł., Pilski, A., Muszyńska, J. (Eds.), 2012. Morasko – the largest iron meteorite shower in Central Europe. Studia i Prace z Geografii i Geologii, 28. Bogucki Wydawnictwo Naukowe.

Pazdur, M., Stankowski, W., Tobolski, K., 1980. Litologiczna i stratygraficzna charakterystyka profilu z kopalnymi utworami organogenicznymi w Malińcu koło Konina (doniesienie wstępne). Badania Fizjograficzne nad Polską Zachodnią, Ser. A, 23, 79–88.
Piotrowski, J.A., Kraus, A.M., 1997. Response of sediment to ice-sheet loading in northwestern Germany: effective stresses and glacier-bed stability. J Glaciol, 43(145), 495–502.
Piotrowski, J.A., Larsen, N.K., Junge, F.W., 2004. Reflections on soft subglacial beds as a mosaic of deforming and stable spots. Quaternary Sci Rev, 23(9–10), 993–1000.
Piotrowski, J.A., Larsen, N.K., Menzies, J., Wysota, W., 2006. Formation of subglacial till under transient bed conditions: deposition, deformation, and basal decoupling under a Weichselian ice sheet lobe, central Poland. Sedimentology, 53(1), 83–106.
Pleskot, K., Tjallingii, R., Makohonienko, M., Nowaczyk, N., Szczuciński, W., 2018. Holocene paleohydrological reconstruction of Lake Strzeszyńskie (western Poland) and its implications for the central European climatic transition zone. J Paleolimnol, 59(4), 443–459.
Pluczyński, A., Sydow, M., 1993. Szczegółowa Mapa Geologiczna Polski. Arkusz Duszniki. PIG, Warszawa.
Pokrzywnicki, J., 1964. Meteorites of Poland (in Polish with English summary). Studia Geologica Polonica, 15(9–140).
Przybylski, B., 2008. Geomorphic traces of a Weichselian ice stream in the Wielkopolska Lowland, western Poland. Boreas, 37(2), 286–296.
Punkari, M., 1997. Glacial and glaciofluvial deposits in the interlobate areas of the Scandinavian Ice Sheet. Quaternary Sci Rev, 16(7), 741–753.
Rinterknecht, V., Börner, A., Bourlès, D., Braucher, R., 2014. Cosmogenic 10Be dating of ice sheet marginal belts in Mecklenburg–Vorpommern, Western Pomerania (northeast Germany). Quat Geochronol, 19, 42–51.
Rinterknecht, V.R., Marks, L., Piotrowski, J.A., Raisbeck, G.M., Yiou, F., Brook, E.J., Clark, P.U., 2005. Cosmogenic Be–10 ages on the Pomeranian Moraine, Poland. Boreas, 34(2), 186–191. Doi 10.1080/03009480510012926
Roman, M., 2017. Ice-flow directions of the last Scandinavian Ice Sheet in central Poland. Quaternary International.
Rotnicki, K., 1960. Oz Bukowsko–Mosinski (The Buk–Mosina Esker). Prace Kom. Geogr. Geol. Pozn. Tow. Przyj. Nauk II (2).
Rotnicki, K., Borówka, R., 1989. Osady górnego plenivistulianu w dolinie dolnej Prosny pod Macewem a wiek maksymalnego zasięgu ostatniego zlodowacenia podczas fazy leszczyńskiej. Badania Fizjograficzne nad Polską Zachodnią A, 40, 5–20.
Spagnolo, M., Phillips, E., Piotrowski, J.A., Rea, B.R., Clark, C.D., Stokes, C.R., Carr, S.J., Ely, J.C., Ribolini, A., Wysota, W., Szuman, I., 2016. Ice stream motion facilitated by a shallow-deforming and accreting bed. Nature communications, 7, 10723.
Stankowska, A., Stankowski, W., 1988. Maximum extent of the Vistulian ice sheet in the vicinity of Konin, Poland: a geomorphological, sedimentological and radiometric evidence. Geographia Polonica, 55, 141–150.
Stankowska, A., Stankowski, W., 1991. Morfo- lito- i chronostratygrafia vistulianu we wschodniej Wielkopolsce. In: K. A. (Ed.), Geneza, litologia i stratygrafia utworów czwartorzedowych. Geografia. Wydawnictwo Naukowe UAM, Poznań, pp. 563–571.
Stankowski, W., 2000. The geological, paleobotanical and radiometric dating of Quaternary sediments in the region of Konin (eastern Great Poland Lowland). Geologos, 5, 175–188.
Stankowski, W., 2001. The geology and morphology of the natural reserve "Meteoryt Morasko". Planetary and Space Science, 49(7), 749–753.
Stankowski, W., 2008. Meteoryt Morasko, osobliwość obszaru Poznania – Morasko meteorite, a curiosity of the Poznań region. Geologia, 19. Wydawnictwo Naukowe UAM, Poznań.
Stokes, C.R., Clark, C.D., Lian, O.B., Tulaczyk, S., 2007. Ice stream sticky spots: A review of their identification and influence beneath contemporary and palaeo-ice streams. Earth-Sci Rev, 81(3–4), 217–249.
Szczuciński, W., Szokaluk, M., Bronikowska, M., Jagodziński, R., Muszyński, A., Wünnemann, K., 2016. Identification and dating of small impact crater ejecta deposits, case of Morasko craters, Poland, 32nd IAS International Meeting of Sedimentology Marrakech, Morocco.
Szewczyk, J., 2010. Geophysical and hydrogeological aspects of utilization of geothermal energy in Poland. Prz Geol, 58(7), 566–573.
Szewczyk, J., Gientka, D., 2009. Terrestrial heat flow density in Poland-a new approach. Geol Q, 53(1), 125–140.
Szokaluk, M., Jagodziński, R., Muszyński, A., Szczuciński, W., 2019. Geology of the Morasko craters, Poznań, Poland—Small impact craters in unconsolidated sediments. Meteorit Planet Sci.

Szuman, I., Ewertowski, M., Kasprzak, L., 2013. Thermo-mechanical facies representative of fast and slow flowing ice sheets: the Weichselian ice sheet, a central west Poland case study. P Geologist Assoc, 124(5), 818–833. 10.1016/j.pgeola.2012.09.003

Szuman, I., Kalita, J.Z., Ewertowski, M.W., 2018. The impact of geothermal heat flux on the last Scandinavian ice sheet over W Poland and E Germany. Geografiska Annaler: Series A, Physical Geography, 100(4), 388–403. 10.1080/04353676.2018.1524711

Thomason, J.F., Iverson, N.R., 2006. Microfabric and microshear evolution in deformed till. Quaternary Sci Rev, 25(9–10), 1027–1038.

Tobolski, K., Mojski, J., 1979a. Biostratigraphy of the Late Pleistocene (Neo-Pleistocene) in the Konin neighbourhood, Symposium on Vistulian Stratigraphy, Poland.

Tobolski, K., Mojski, J., 1979b. Fossil flora in the Maliniec site. Vistulian.

van der Meer, J.J., Menzies, J., Rose, J., 2003. Subglacial till: the deforming glacier bed. Quaternary Sci Rev, 22(15–17), 1659–1685.

Waller, R.I., Murton, J.B., Knight, P.G., 2009. Basal glacier ice and massive ground ice: different scientists, same science? Geological Society, London, Special Publications, 320(1), 57–69.

Włodarski, W., Papis, J., Szczuciński, W., 2017. Morphology of the Morasko crater field (western Poland): Influences of pre-impact topography, meteoroid impact processes, and post-impact alterations. Geomorphology, 295, 586–597.

Woldstedt, P., 1925. Die großen Endmoränenzüge Norddeutschlands. Zeitschrift der Deutschen Geologischen Gesellschaft, 172–184.

Woldstedt, P., 1954. Das Eiszeitalter. Grundlinien einer Geologie des Quartärs. Geologiska Föreningen i Stockholm Förhandlingar, 76(4), 707–707. 10.1080/11035895409453589

Wysota, W., Molewski, P., Sokołowski, R.J., 2009. Record of the Vistula ice lobe advances in the Late Weichselian glacial sequence in north-central Poland. Quaternary International, 207(1–2), 26–41.

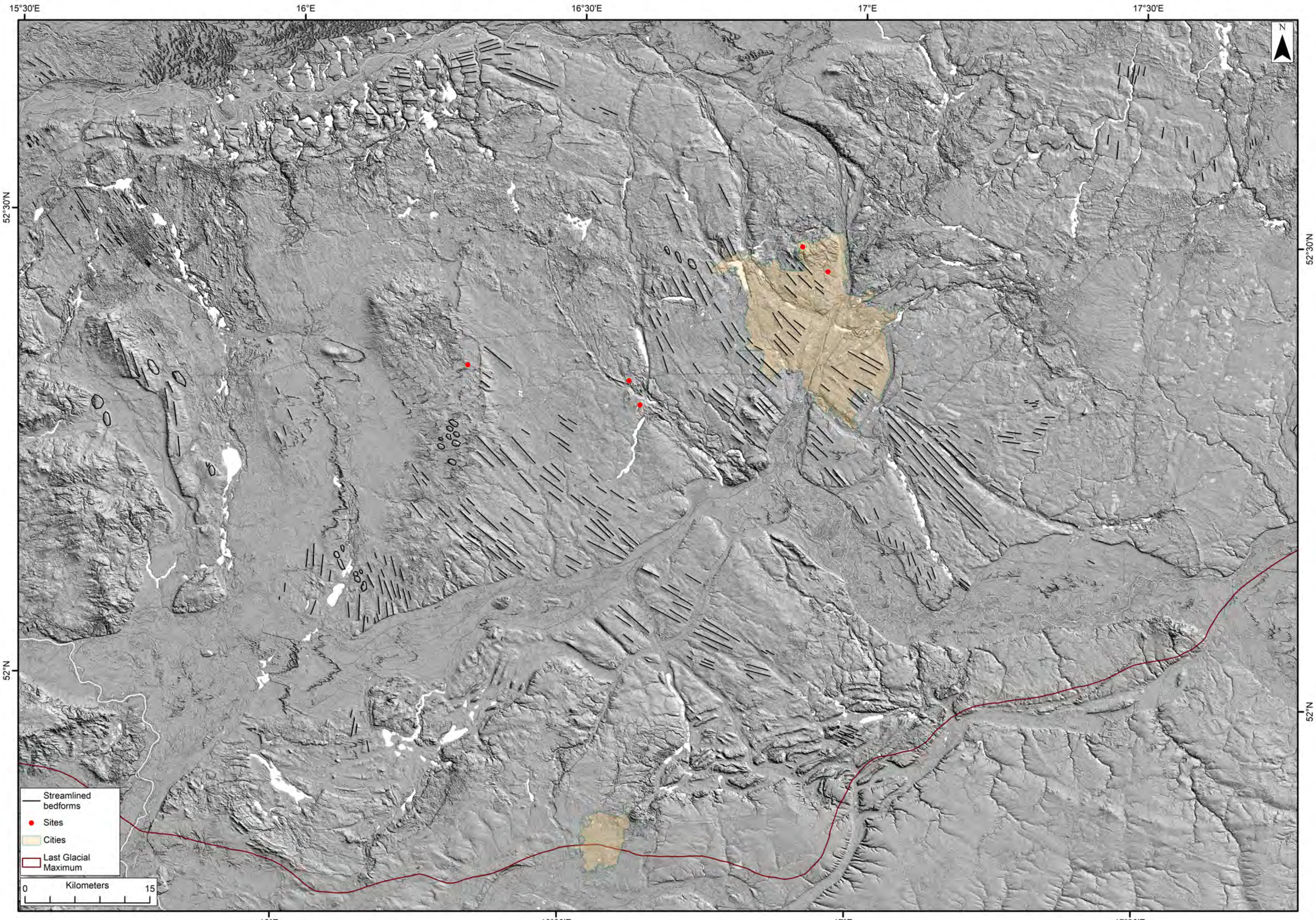
15°30'E
16°E
16°30'E
17°E
17°30'E
52°30'N
52°N
N
Streamlined bedforms
Sites
Cities
Last Glacial Maximum
Kilometers
0
15

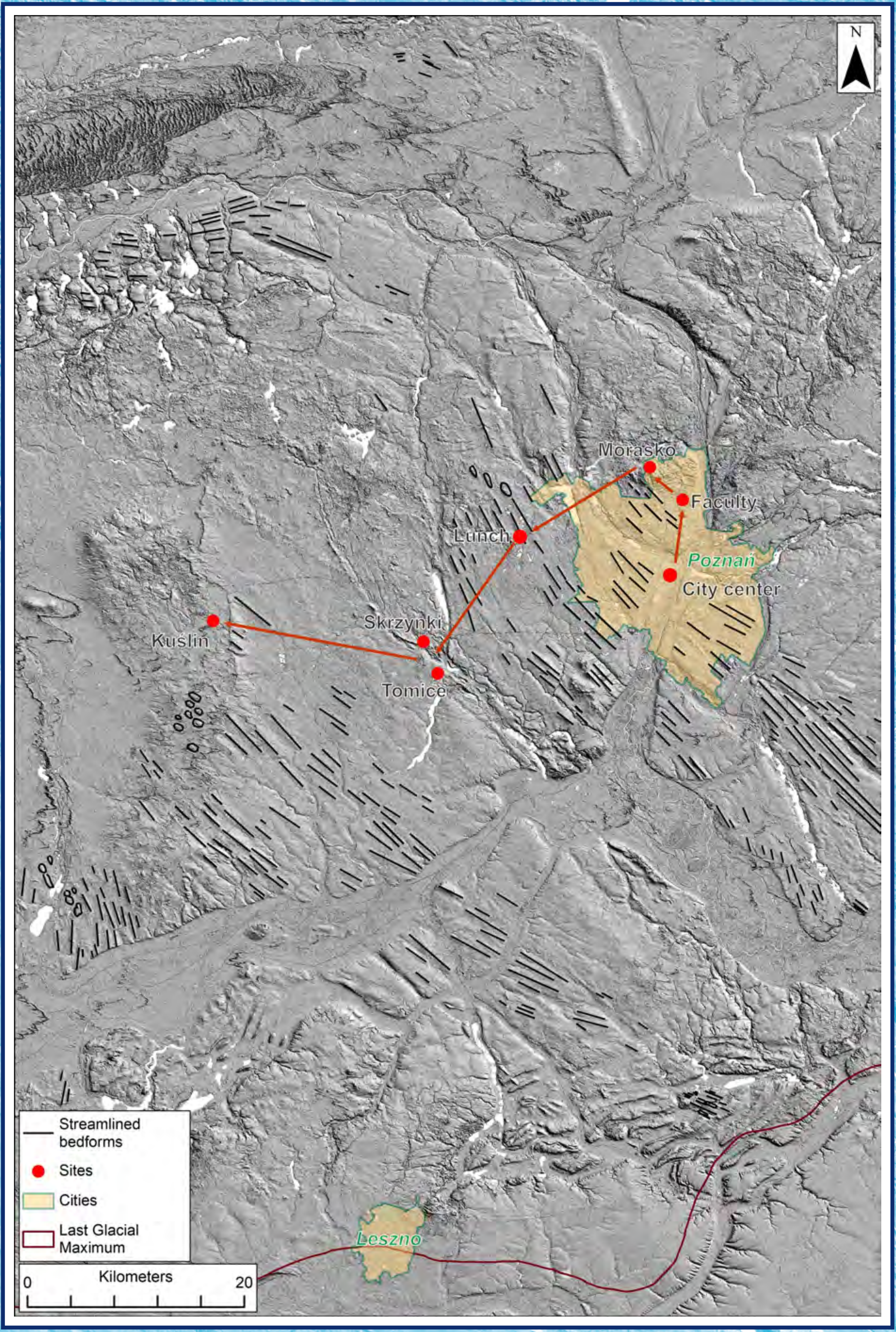

Bogucki
WYDAWNICTWO NAUKOWE

ISBN 978-83-7986-243-6